

Supplementary Material

RSC Advances

Stereospecific Alkylation of Substituted Adenines by the Mitsunobu Coupling Reaction under Microwave- Assisted Conditions

María E. García-Rubiño,^a María C. Núñez,^a Duane Choquesillo-Lazarte,^b

Juan M. García-Ruiz,^b Yolanda Madrid,^c Joaquín M. Campos,^{a*}

^a*Departamento de Química Farmacéutica y Orgánica, Facultad de Farmacia, c/ Campus de Cartuja, s/n, 18071*

Granada (Spain)

^b*Laboratorio de Estudios Cristalográficos, Instituto Andaluz de Ciencias de la Tierra (UGR - CSIC), Avenida de las*

Palmeras N° 4, E-18100 Armilla, Granada (Spain)

^c*Centro de Instrumentación Científica, Universidad de Granada, Edificio Mecenas. Campus Universitario de Fuente*

Nueva. 18071 Granada (Spain).

INDEX	Page
Figure S1: (<i>RS</i>)- 12	4
Figure S2: (<i>R</i>)- 12	5
Figure S3: (<i>S</i>)- 12	6
Figure S4: (<i>RS</i>)- 13	7
Figure S5: (<i>R</i>)- 13	8
Figure S6: (<i>S</i>)- 13	9
Figure S7: (<i>RS</i>)- 14	10
Figure S8: (<i>S</i>)- 14	11
Figure S9: (<i>RS</i>)- 17	12
Figure S10: (<i>R</i>)- 17	13
Figure S11: (<i>S</i>)- 17	14
Figure S12: (<i>RS</i>)- 18	15
Figure S13: (<i>R</i>)- 18	16
Figure S14: (<i>S</i>)- 18	17
Figure S15: (<i>RS</i>)- 22	18
Figure S16: (<i>R</i>)- 22	19
Figure S17: (<i>S</i>)- 22	20
Figure S18: (<i>RS</i>)- 23	21
Figure S19: (<i>R</i>)- 23	22
Figure S20: (<i>S</i>)- 23	23
Figure S21: (<i>RS</i>)- 24	24
Figure S22: (<i>R</i>)- 24	25
Figure S23: (<i>S</i>)- 24	26
¹ H NMR spectrum of 17 :.....	27
¹³ C NMR spectrum of 17 :.....	28
DEPT spectrum of 17 :.....	29
HSQC spectrum of 17 :.....	30
HMBC spectrum of 17 :.....	31
¹ H NMR spectrum of 18 :.....	32
¹³ C NMR spectrum of 18 :.....	33

DEPT spectrum of 18 :	34
HSQC spectrum of 18 :	35
HMBC spectrum of 18 :	36
¹ H NMR spectrum of 22 :.....	37
¹³ C NMR spectrum of 22 :	38
DEPT spectrum of 22 :	39
HSQC spectrum of 22 :	40
HMBC spectrum of 22 :	41
¹ H NMR spectrum of 23 :.....	42
¹³ C NMR spectrum of 23 :	43
DEPT spectrum of 23 :	44
HSQC spectrum of 23 :	45
HMBC spectrum of 23 :	46
¹ H NMR spectrum of 24 :.....	47
¹³ C NMR spectrum of 24 :	48
DEPT spectrum of 24 :	49
HSQC spectrum of 24 :	50
HMBC spectrum of 24 :	51
Figure S24: Crystal Structure (<i>RS</i>)- 17	52
Figure S25: Crystal Structure (<i>RS</i>)- 17	53
Figure S26: Crystal Structure (<i>R</i>)- 22	54
Figure S27: Crystal Structure (<i>R</i>)- 22	54
Figure S28: Crystal Structure (<i>RS</i>)- 24	55
Figure S29: Crystal Structure (<i>RS</i>)- 24	56

CHIRALPAK IA 250 x 4.6 mm
Flow rate: 1ml/min
room temperature
PDA 250.0 nm
n-hexane/dichloromethane 65/35 v/v

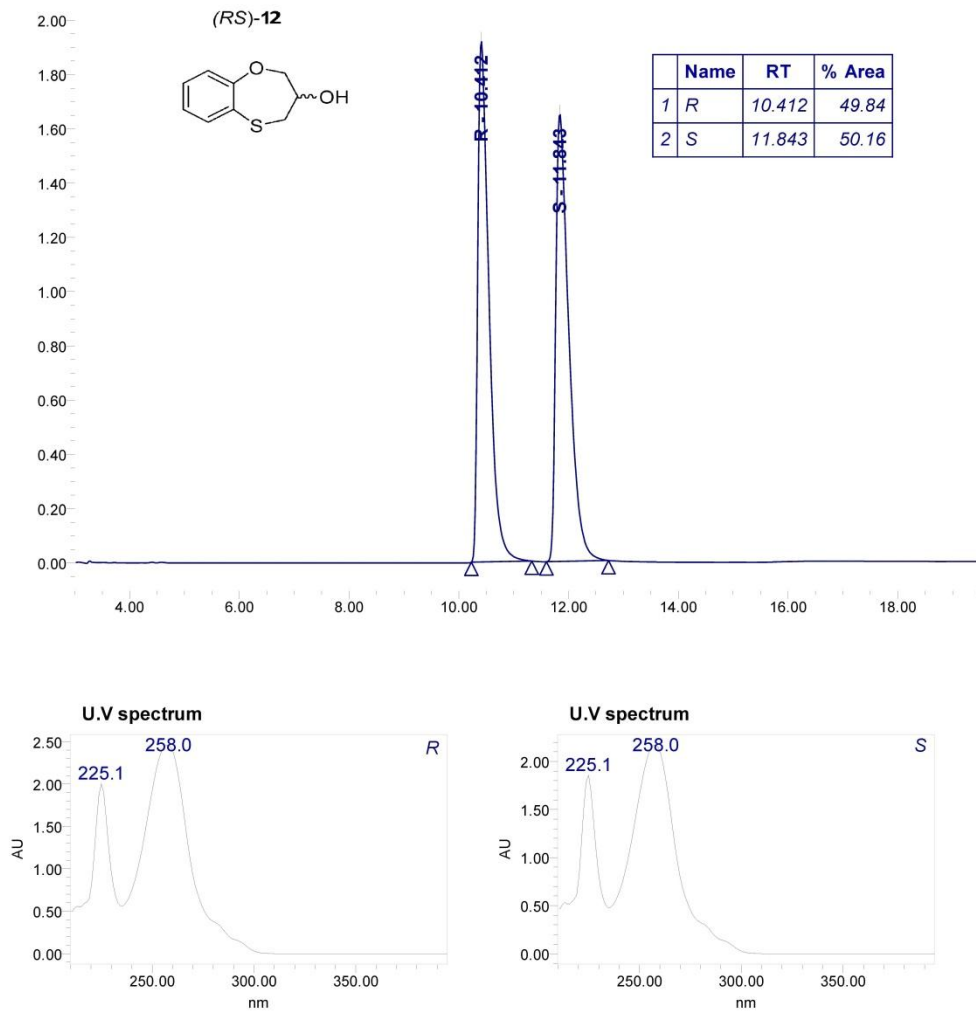


Figure S1

CHIRALPAK IA 250 x 4.6 mm
Flow rate: 1 ml/min
room temperature
PDA 250.0 nm
n-hexane/dichloromethane 65/35 v/v

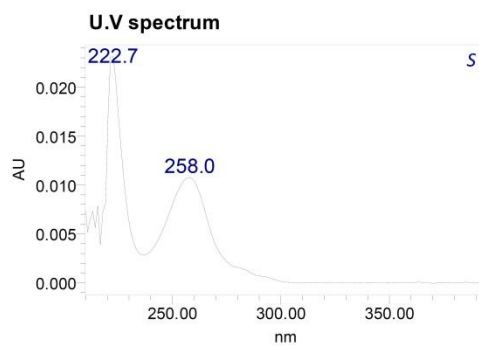
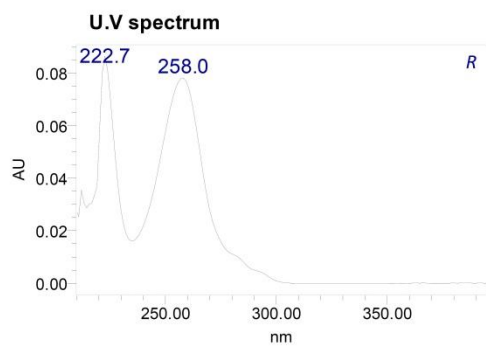
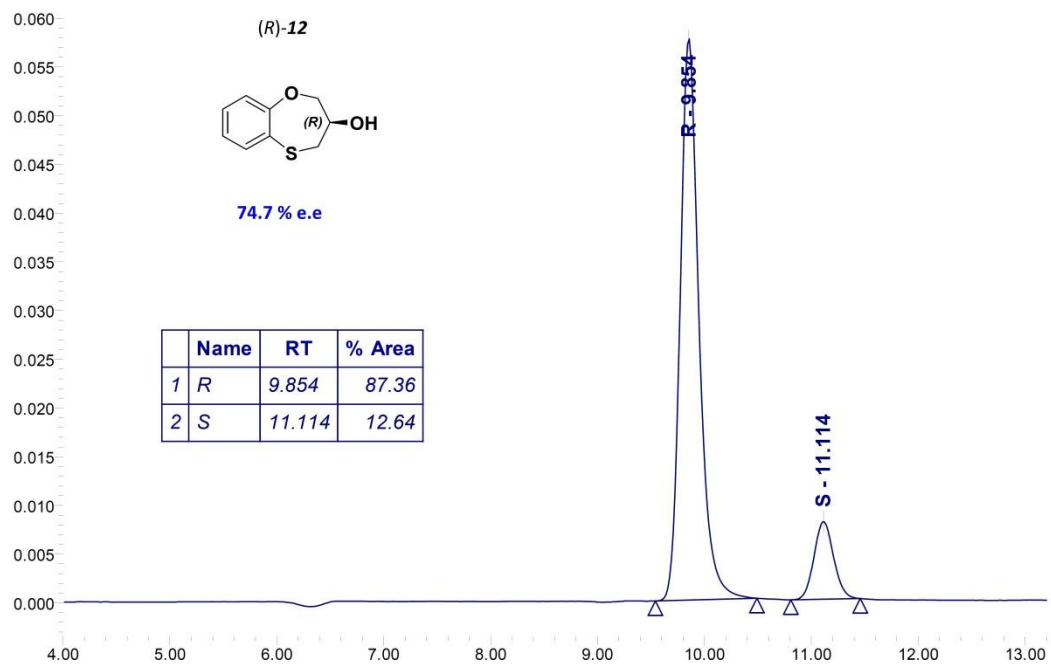


Figure S2

CHIRALPAK IA 250 x 4.6 mm
Flow rate: 1ml/min
room temperature
PDA 250.0 nm
n-hexane/dichloromethane 65/35 v/v

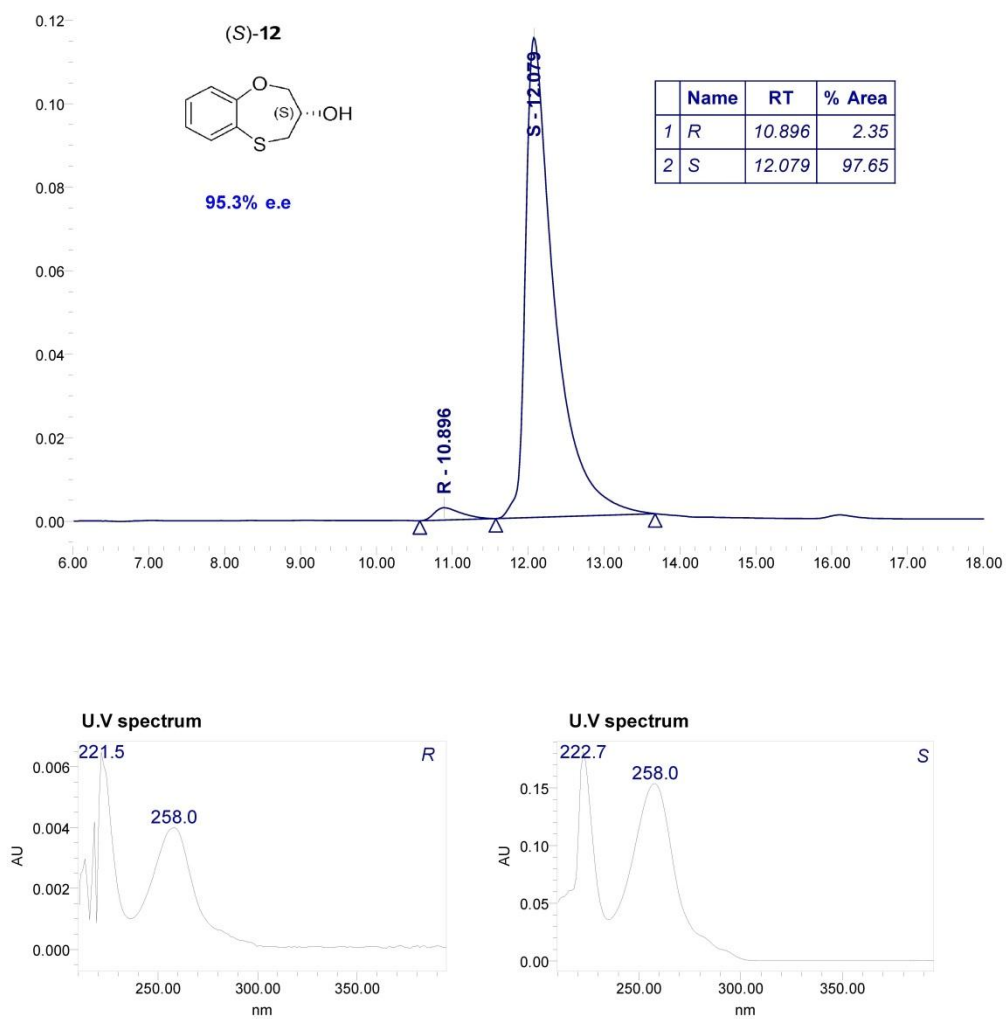


Figure S3

CHIRALPAK IA 250 x 4.6 mm
Flow rate: 1ml/min
room temperature
PDA 250.0 nm
n-hexane/dichloromethane 65/35 v/v

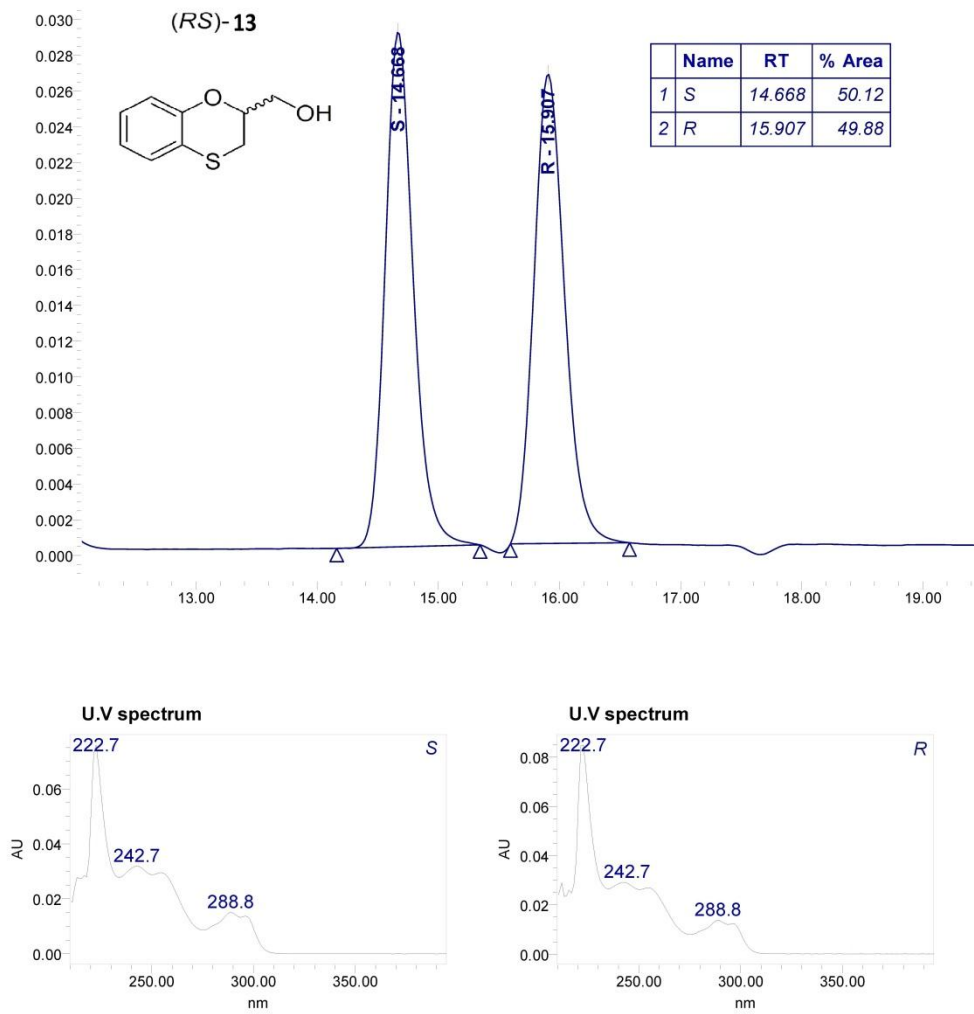


Figure S4

CHIRALPAK IA 250 x 4.6 mm
Flow rate: 1ml/min
room temperature
PDA 250.0 nm
n-hexane/dichloromethane 65/35 v/v

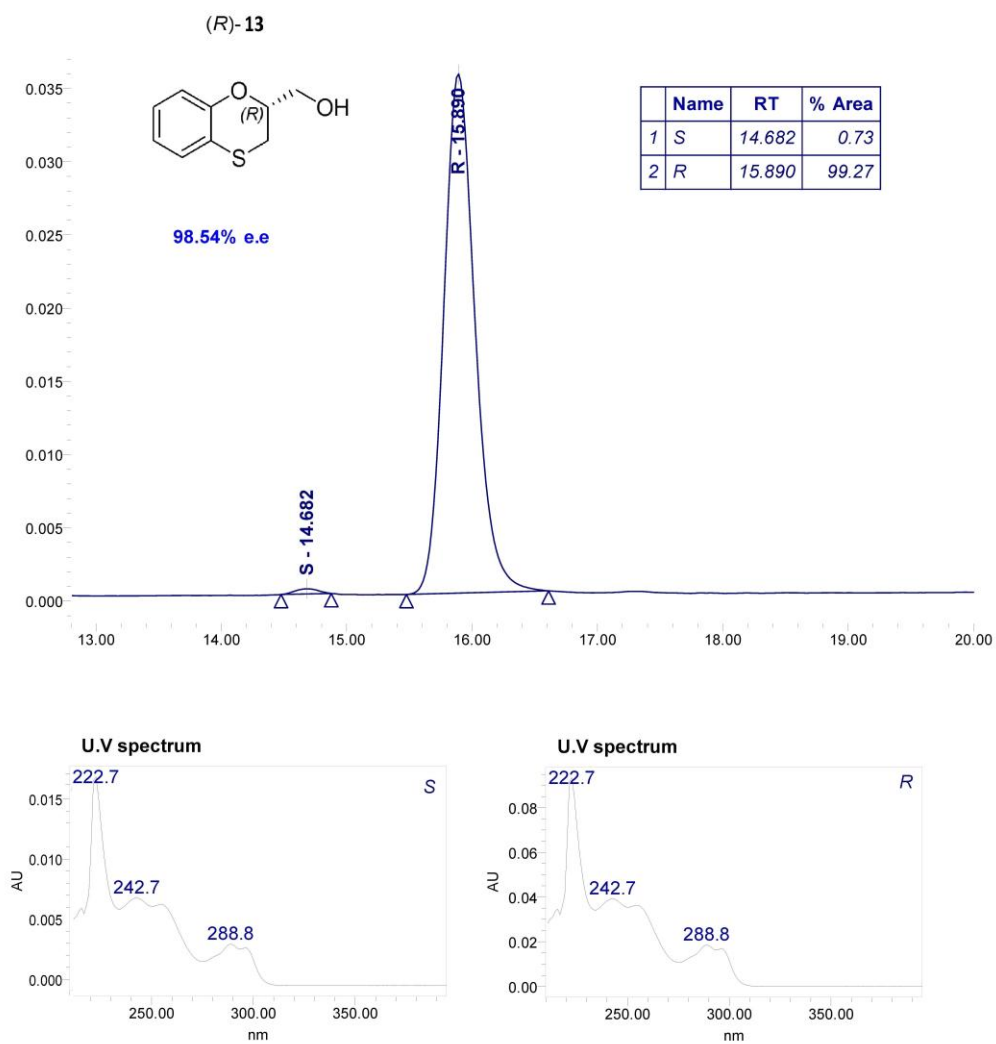


Figure S5

CHIRALPAK IA 250 x 4.6 mm
Flow rate: 1ml/min
room temperature
PDA 250.0 nm
n-hexane/dichloromethane 65/35 v/v

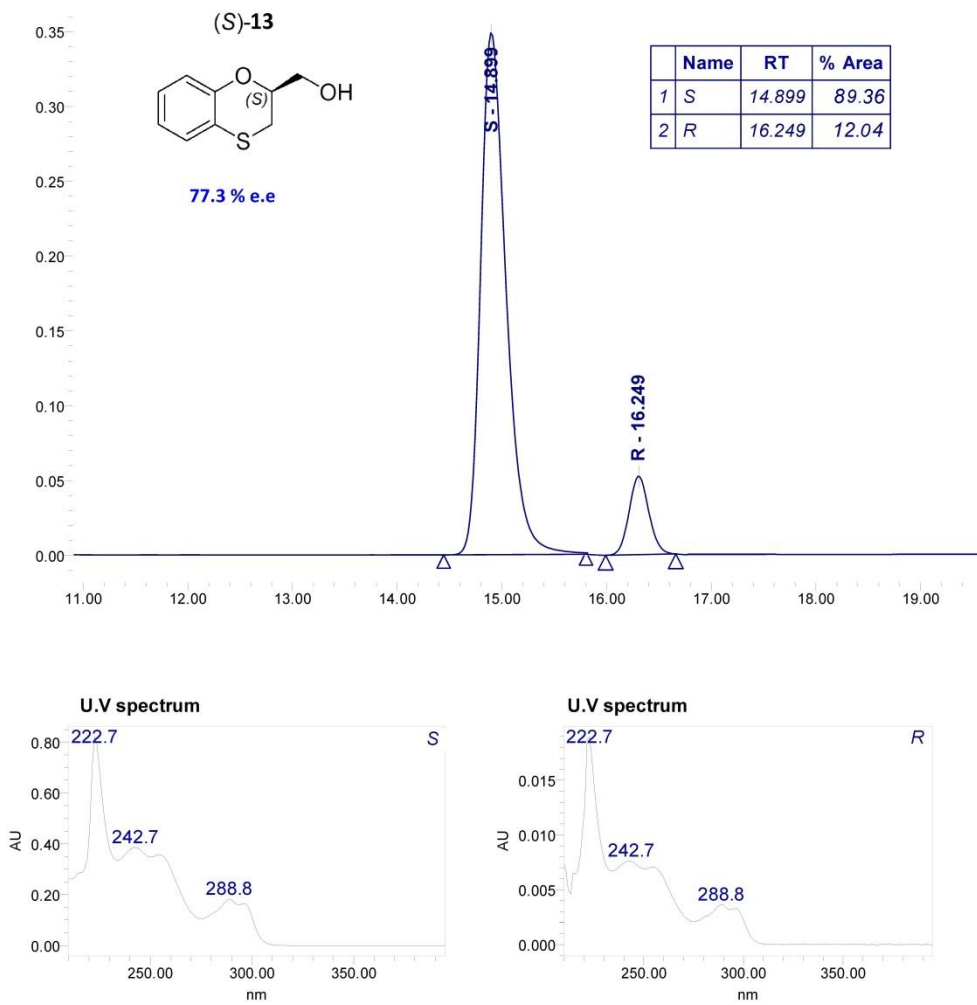


Figure S6

CHIRALPAK IA 250 x 4.6 mm
Flow rate: 1ml/min
room temperature
PDA 250.0 nm
n-hexane/2-propanol 90/10 v/v

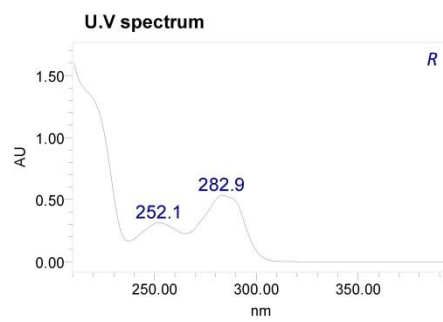
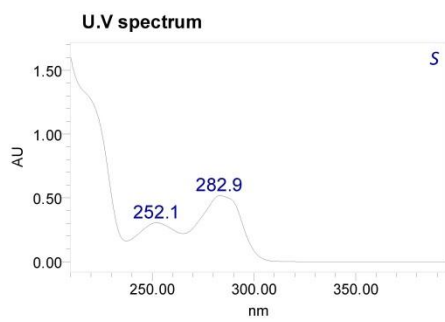
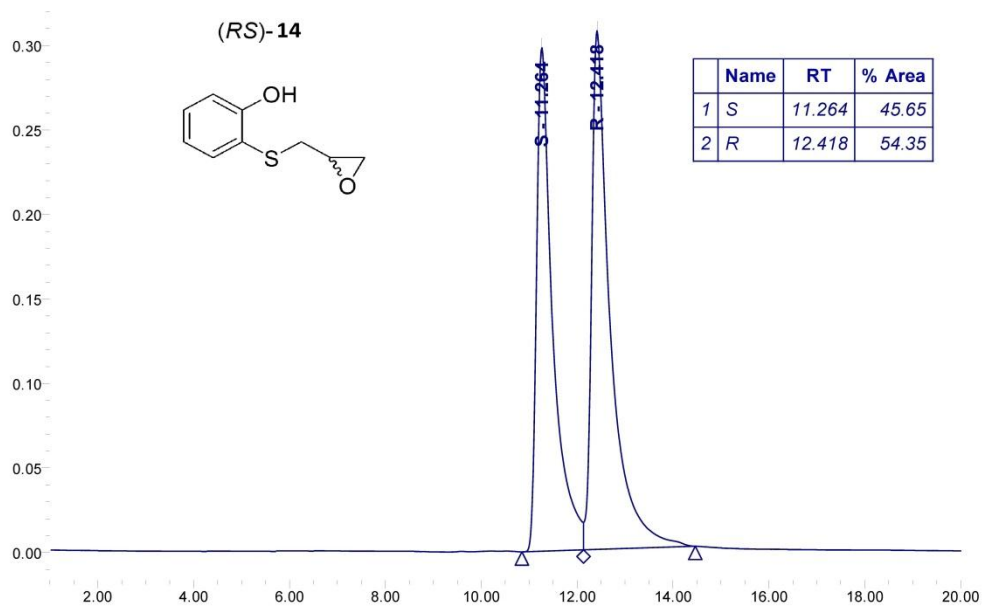


Figure S7

CHIRALPAK IA 250 x 4.6 mm
Flow rate: 1ml/min
room temperature
PDA 250.0 nm
n-hexane/2-propanol 90/10 v/v

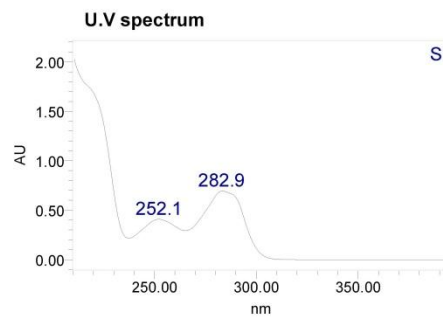
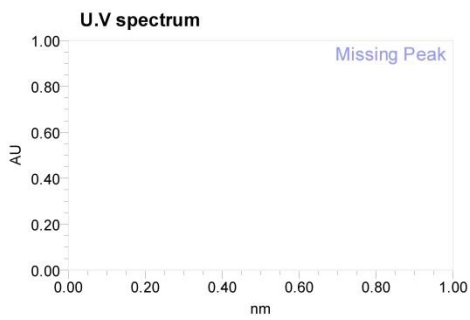
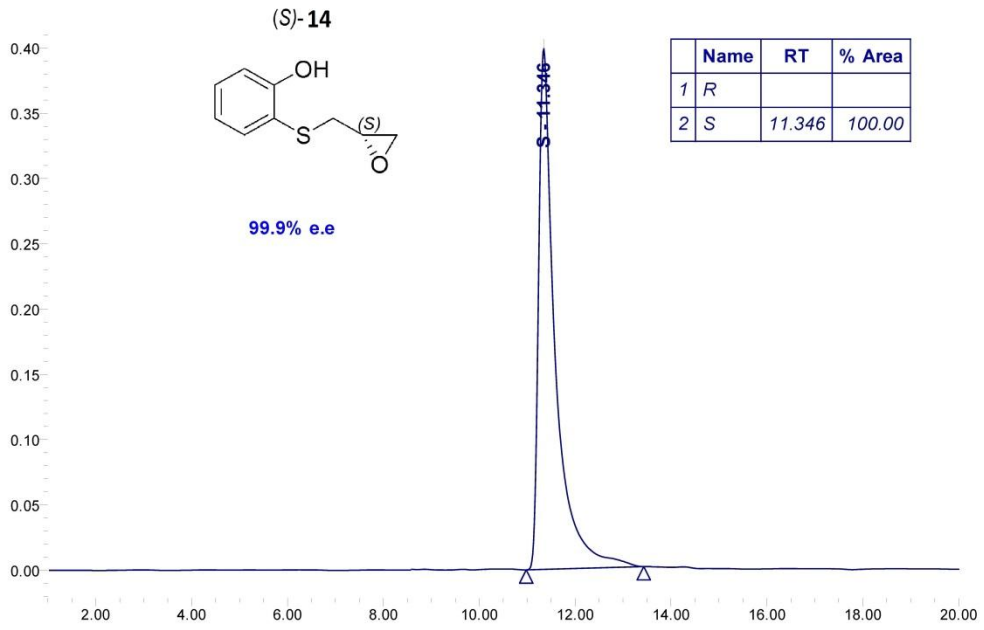


Figure S8

CHIRALPAK IA 250 x 4.6 mm
Flow rate: 1ml/min
room temperature
PDA 250.0 nm
n-hexane/ethanol 80/20 v/v

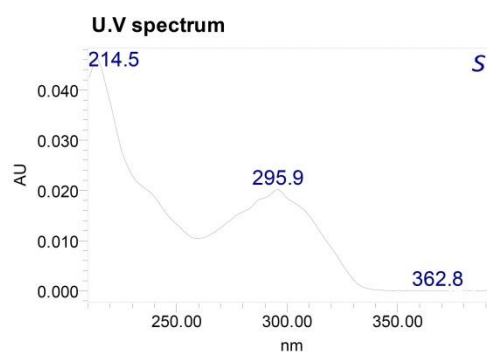
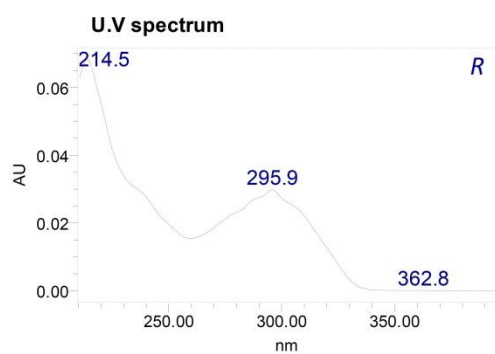
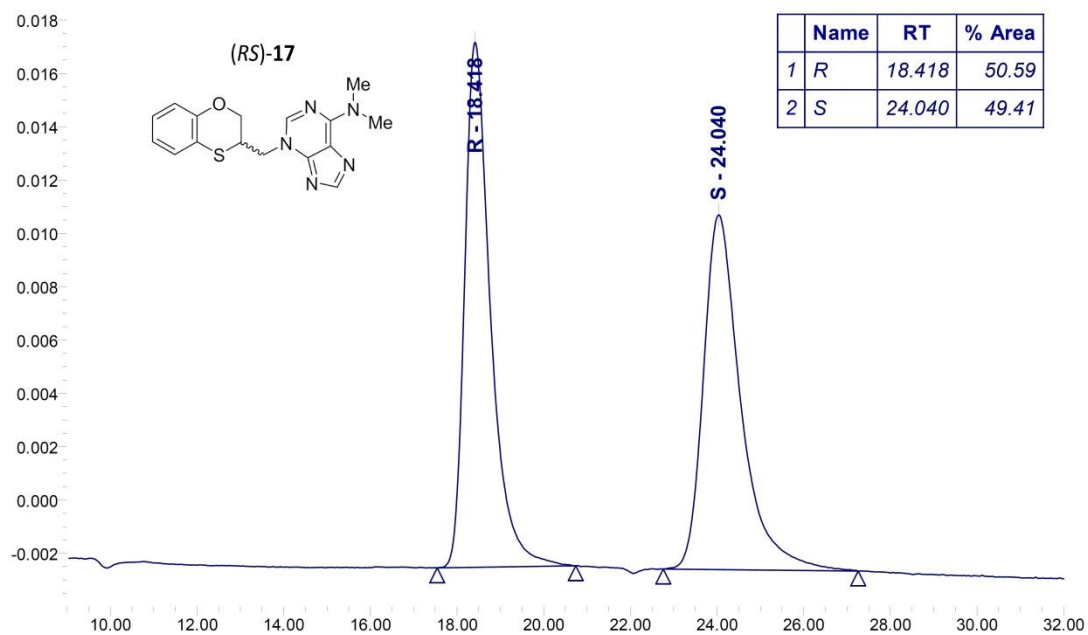


Figure S9

CHIRALPAK IA 250 x 4.6 mm
Flow rate: 1ml/min
room temperature
PDA 250.0 nm
n-hexane/ethanol 80/20 v/v

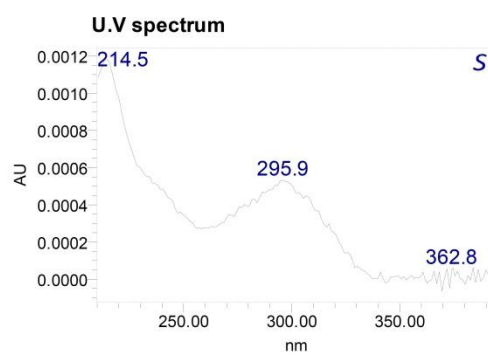
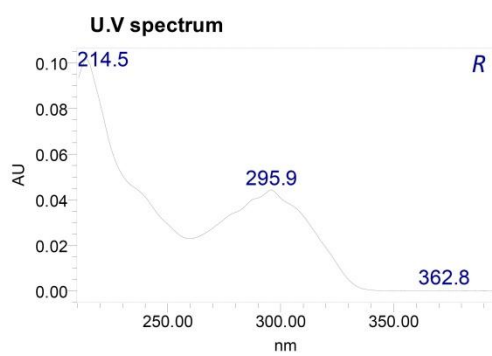
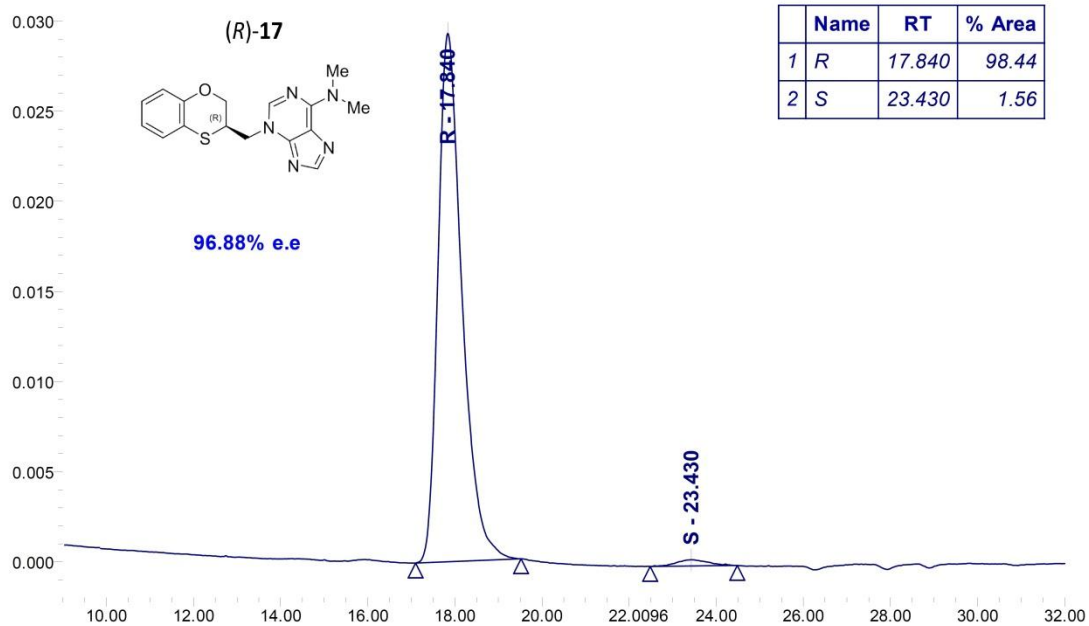


Figure S10

CHIRALPAK IA 250 x 4.6 mm
Flow rate: 1ml/min
room temperature
PDA 250.0 nm
n-hexane/ethanol 80/20 v/v

	Name	RT	% Area
1	R	18.242	12.00
2	S	23.055	88.00

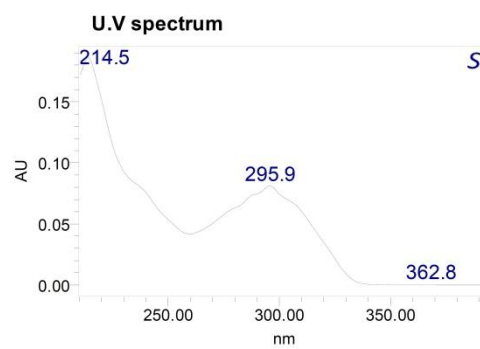
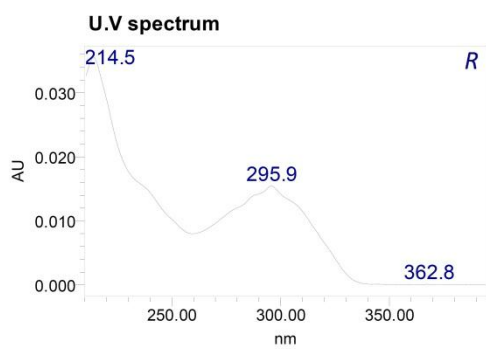
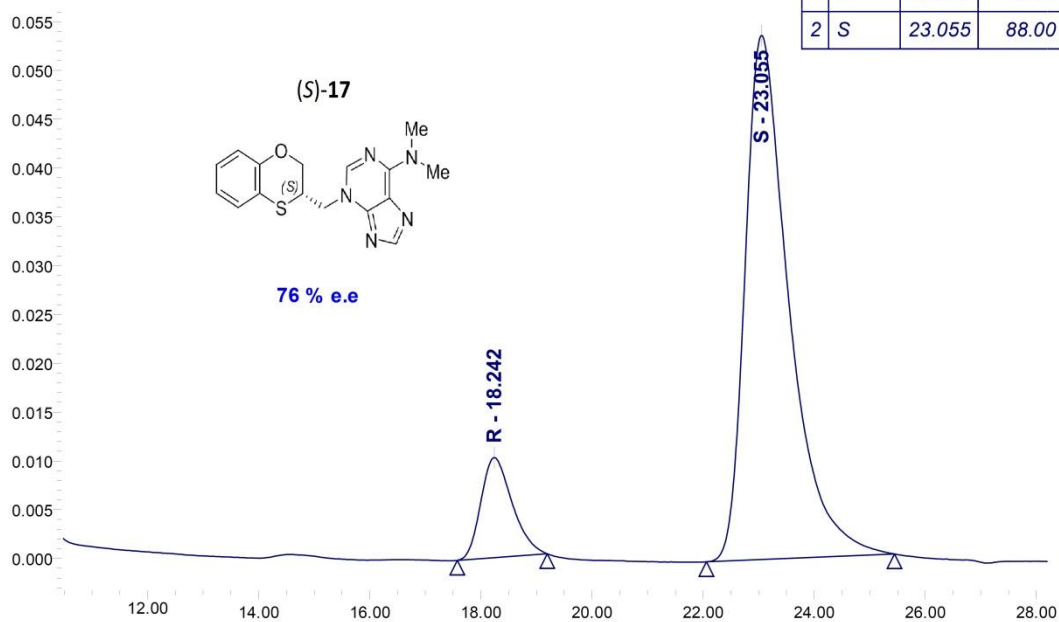


Figure S11

CHIRALPAK IA 250 x 4.6 mm
Flow rate: 1ml/min
room temperature
PDA 250.0 nm
n-hexane/ethanol 80/20 v/v

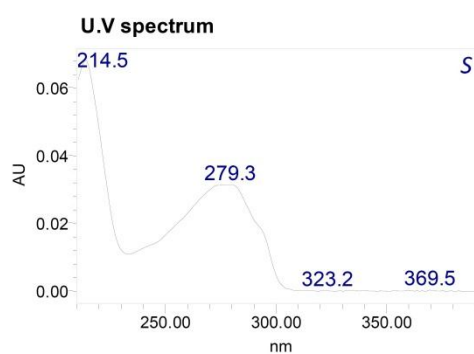
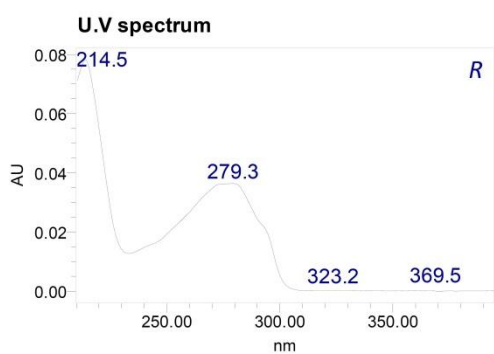
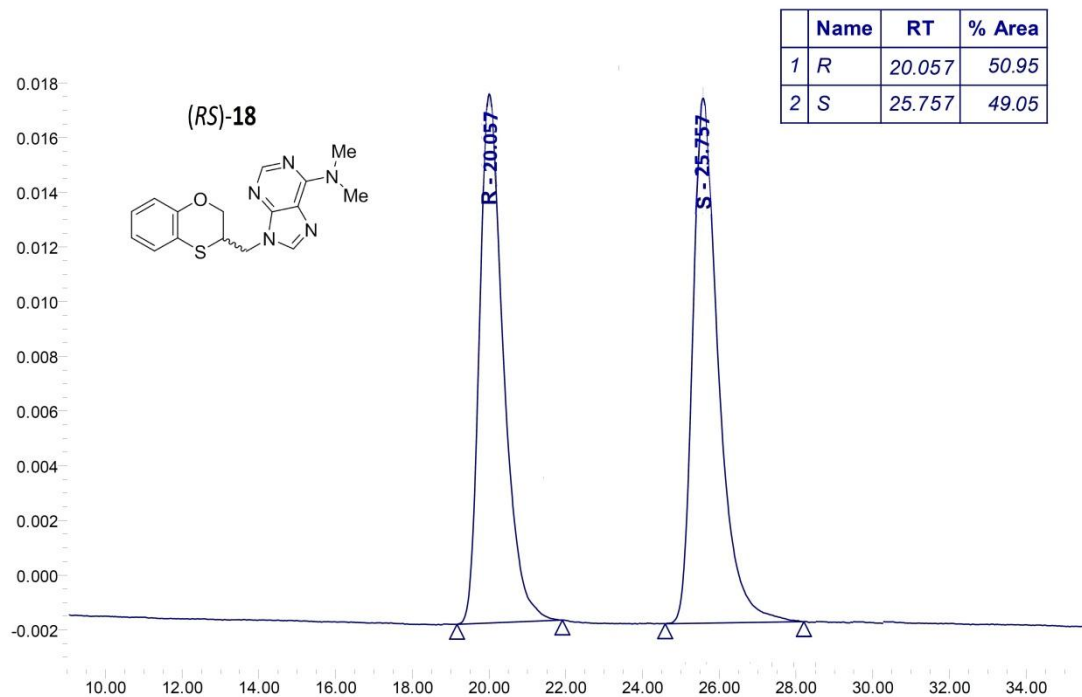


Figure S12

CHIRALPAK IA 250 x 4.6 mm
Flow rate: 1ml/min
room temperature
PDA 250.0 nm
n-hexane/ethanol 80/20 v/v

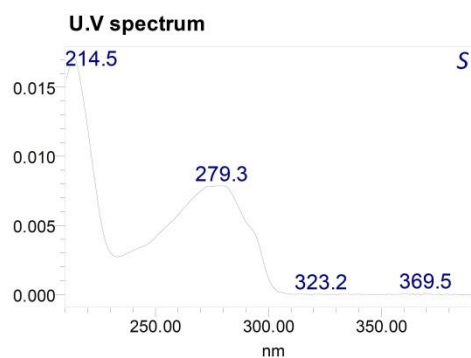
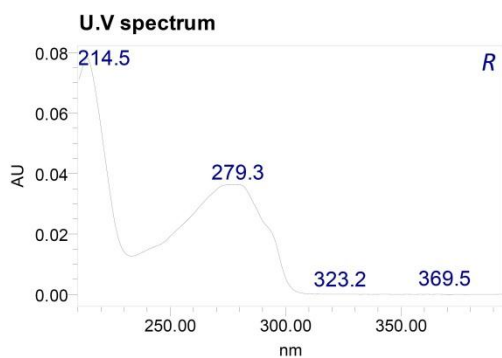
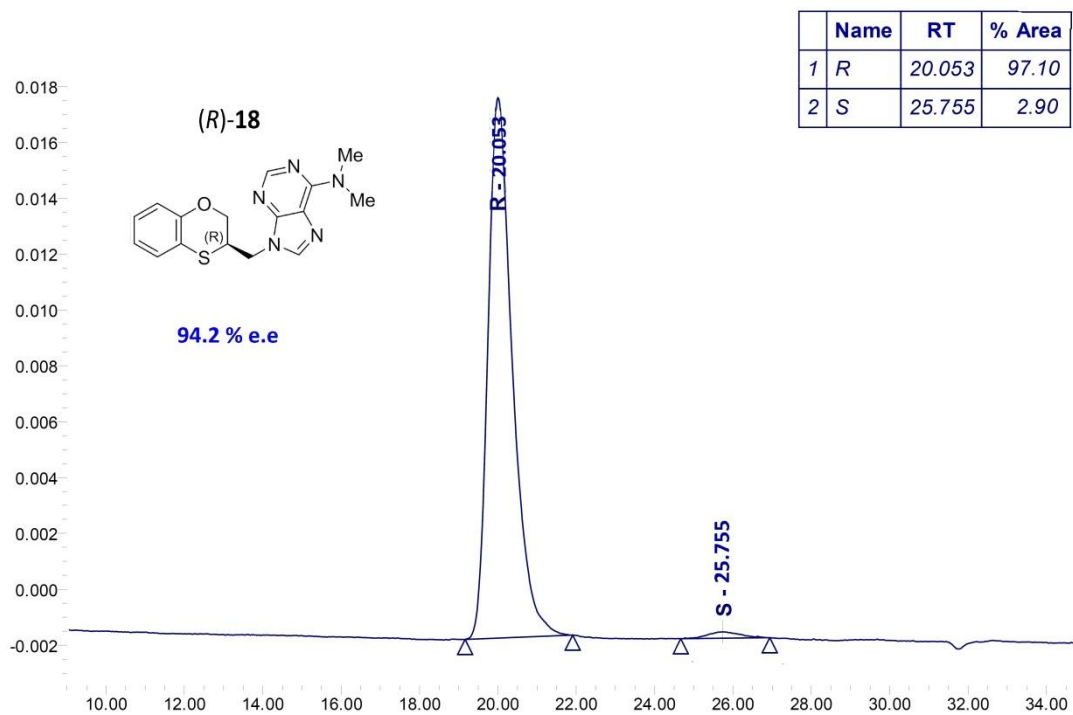


Figure S13

CHIRALPAK IA 250 x 4.6 mm
Flow rate: 1ml/min
room temperature
PDA 250.0 nm
n-hexane/ethanol 80/20 v/v

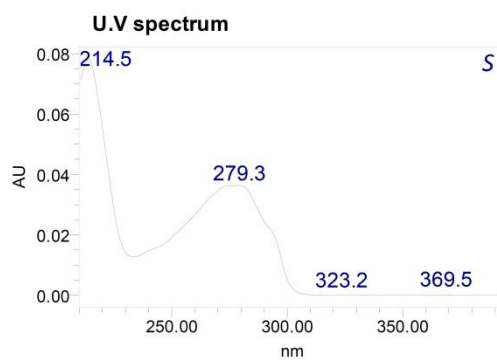
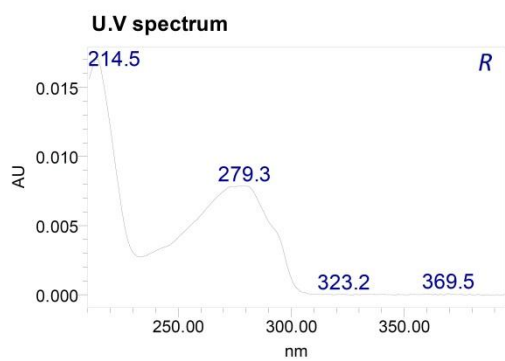
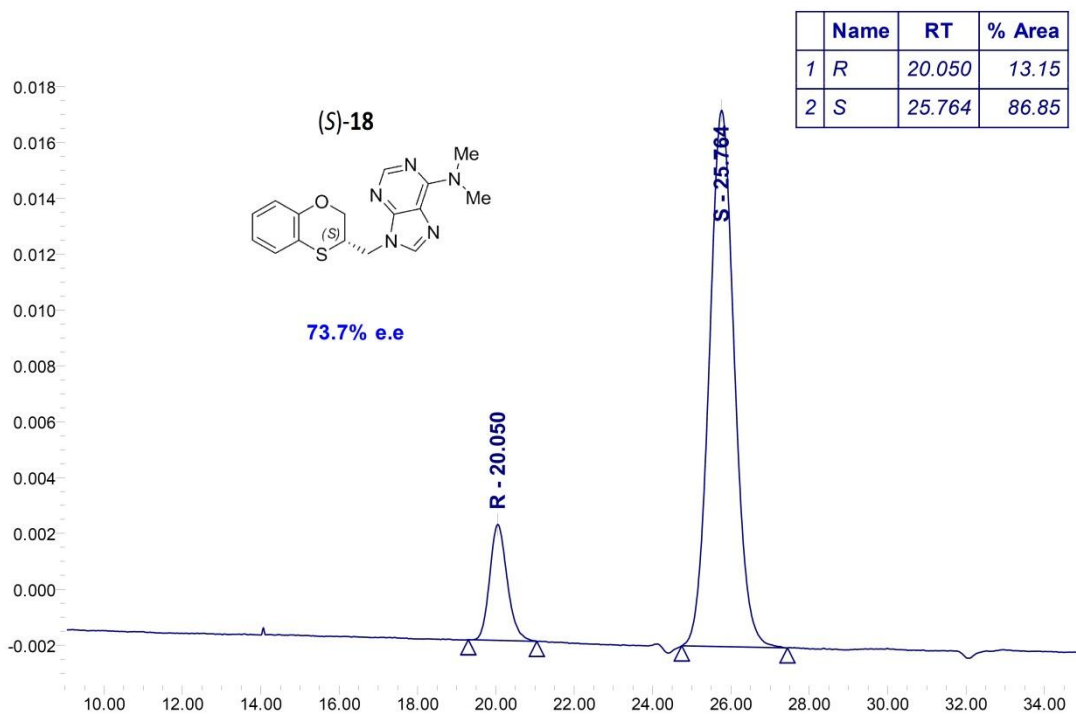


Figure S14

CHIRALPAK IA 250 x 4.6 mm
Flow rate: 1ml/min
room temperature
PDA 250.0 nm
n-hexane/ethanol 80/20 v/v

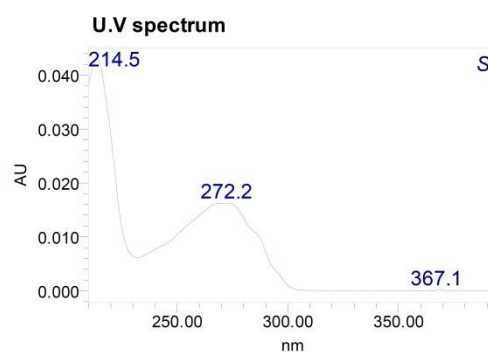
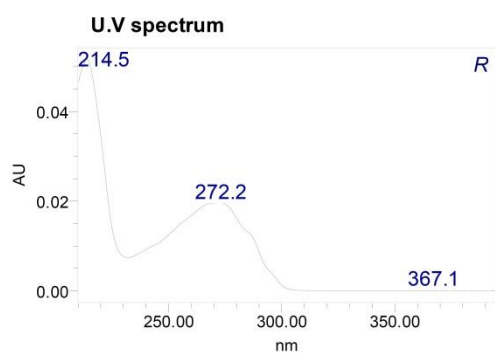
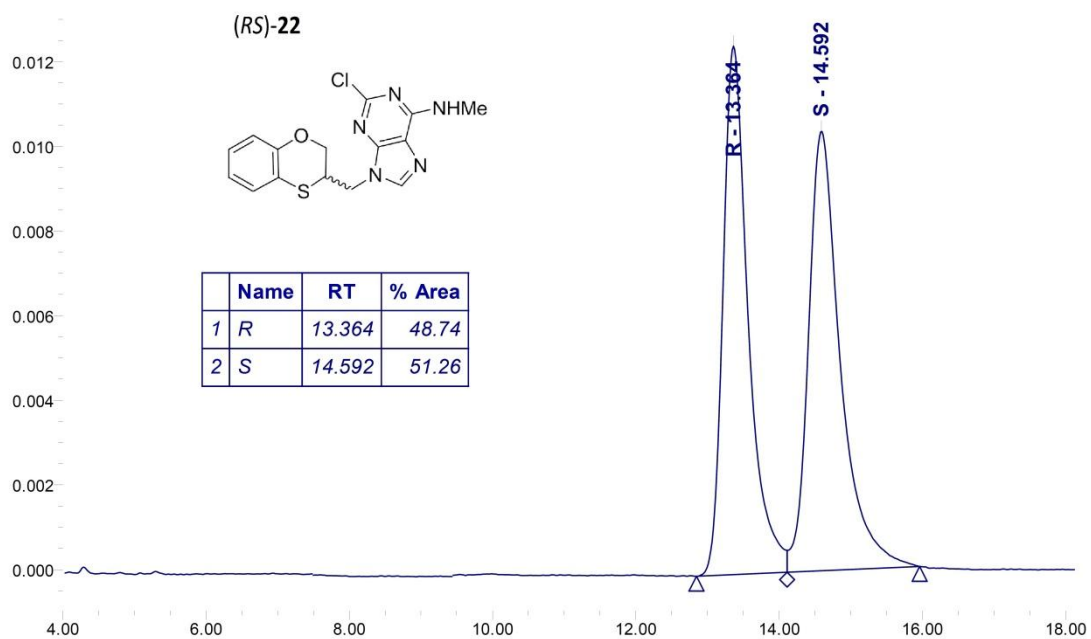


Figure S15

CHIRALPAK IA 250 x 4.6 mm
Flow rate: 1ml/min
room temperature
PDA 250.0 nm
n-hexane/ethanol 80/20 v/v

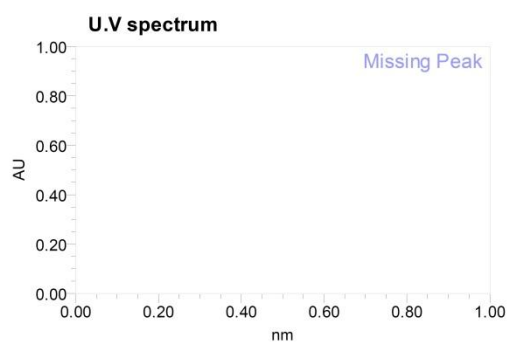
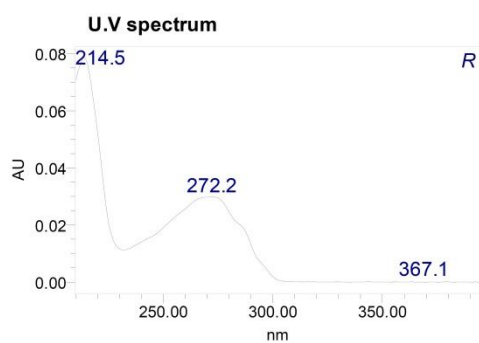
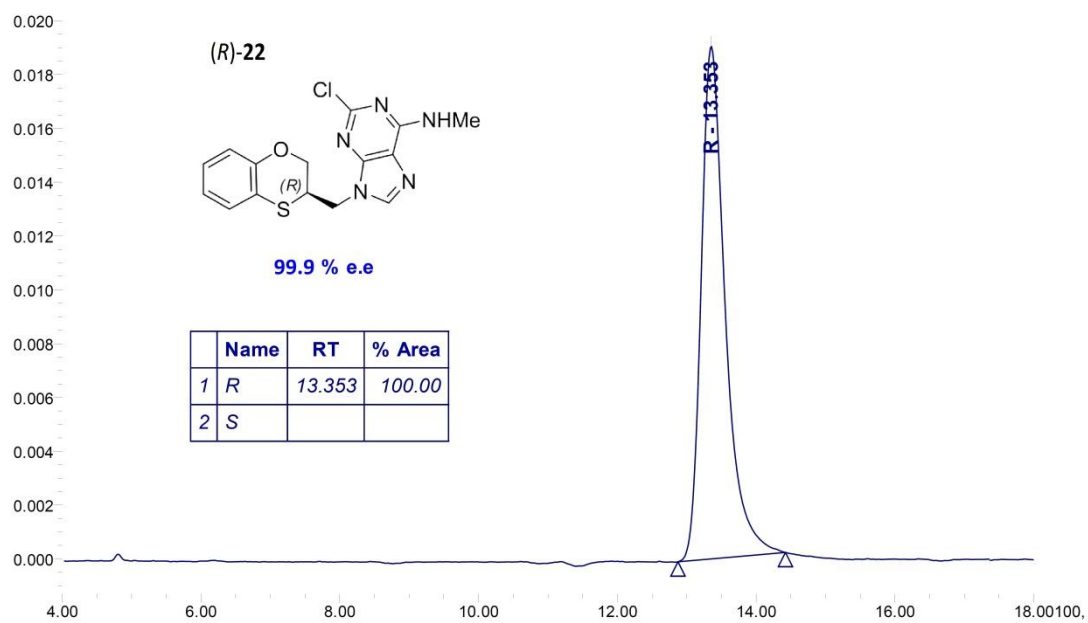


Figure S16

CHIRALPAK IA 250 x 4.6 mm
Flow rate: 1ml/min
room temperature
PDA 250.0 nm
n-hexane/ethanol 80/20 v/v

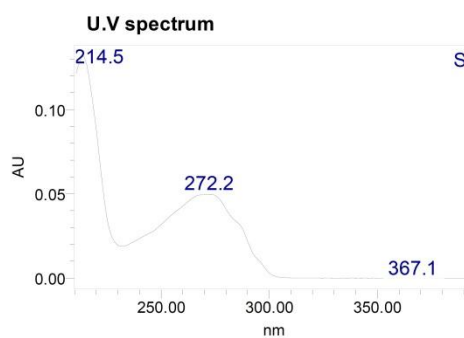
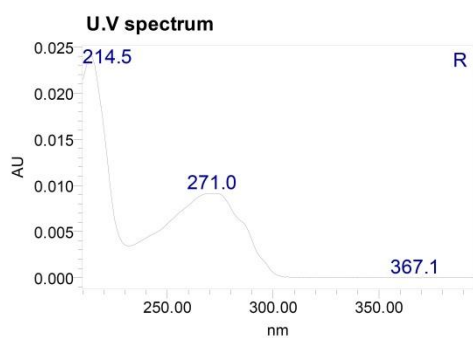
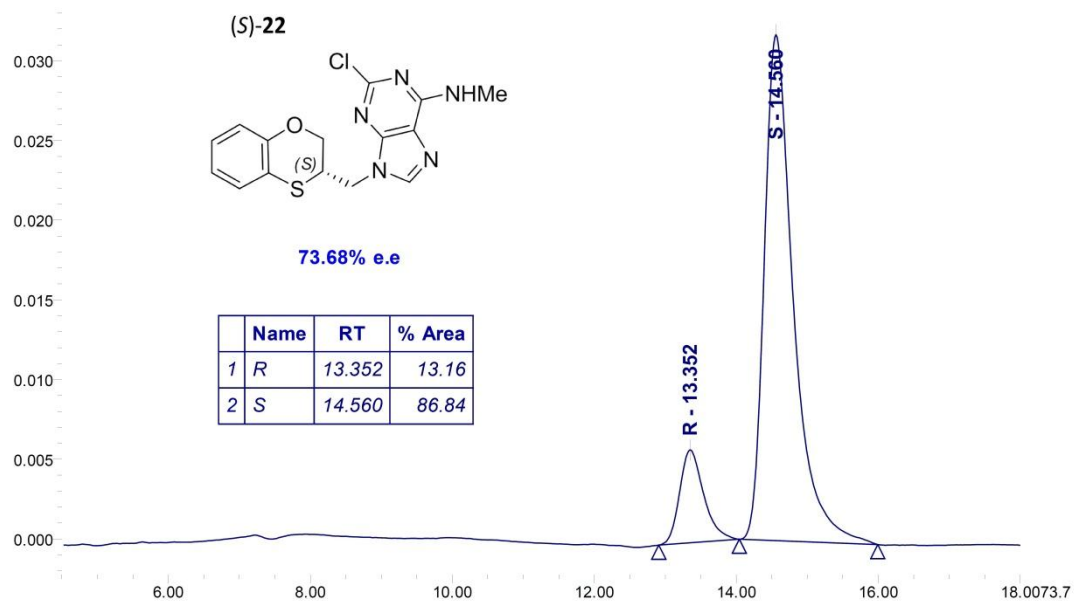


Figure S17

CHIRALPAK IA 250 x 4.6 mm
Flow rate: 1ml/min
room temperature
PDA 250.0 nm
n-hexane/ethanol 80/20 v/v

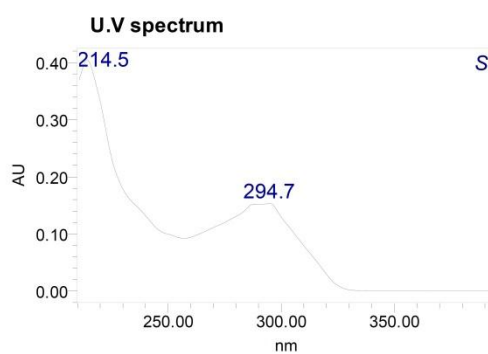
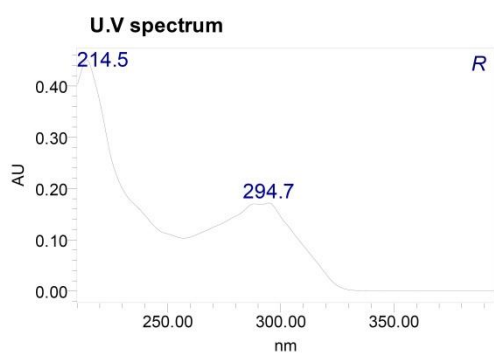
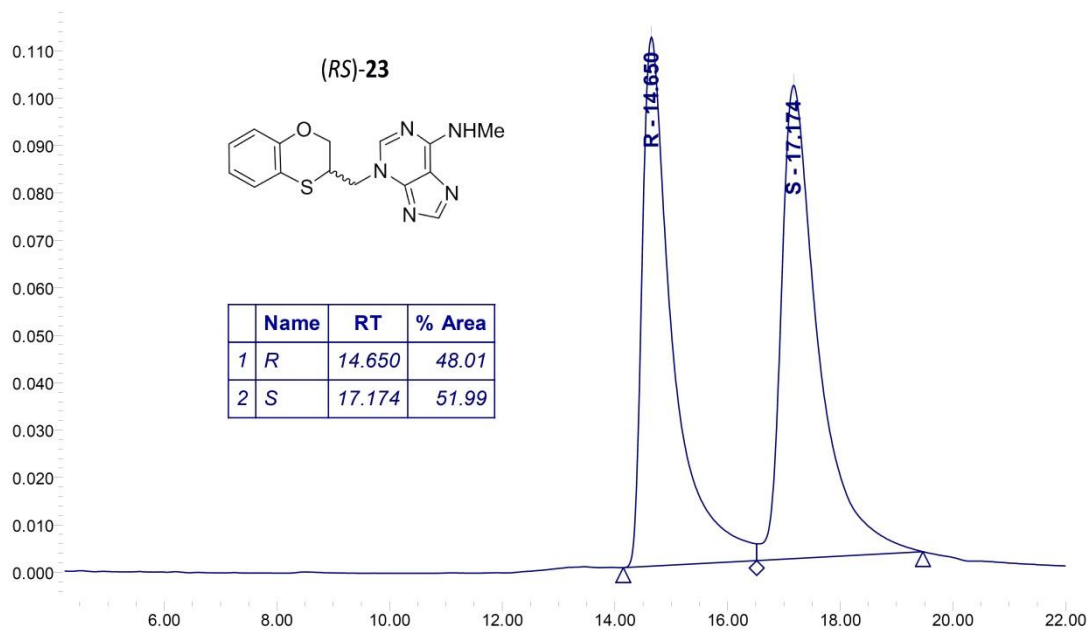


Figure S18

CHIRALPAK IA 250 x 4.6 mm
Flow rate: 1ml/min
room temperature
PDA 250.0 nm
n-hexane/ethanol 80/20 v/v

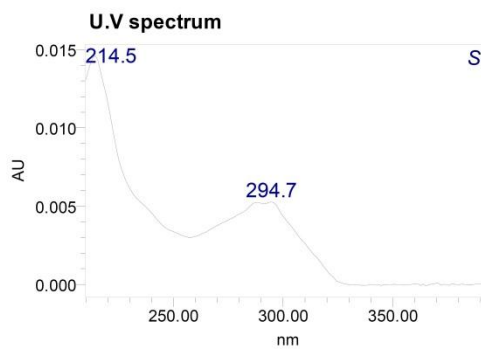
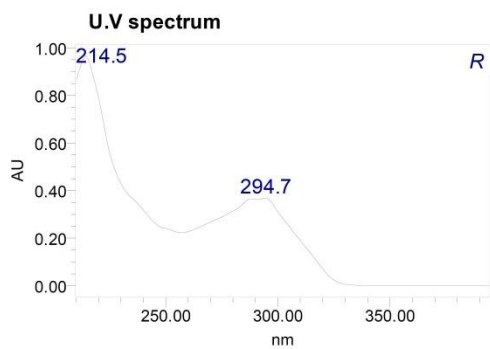
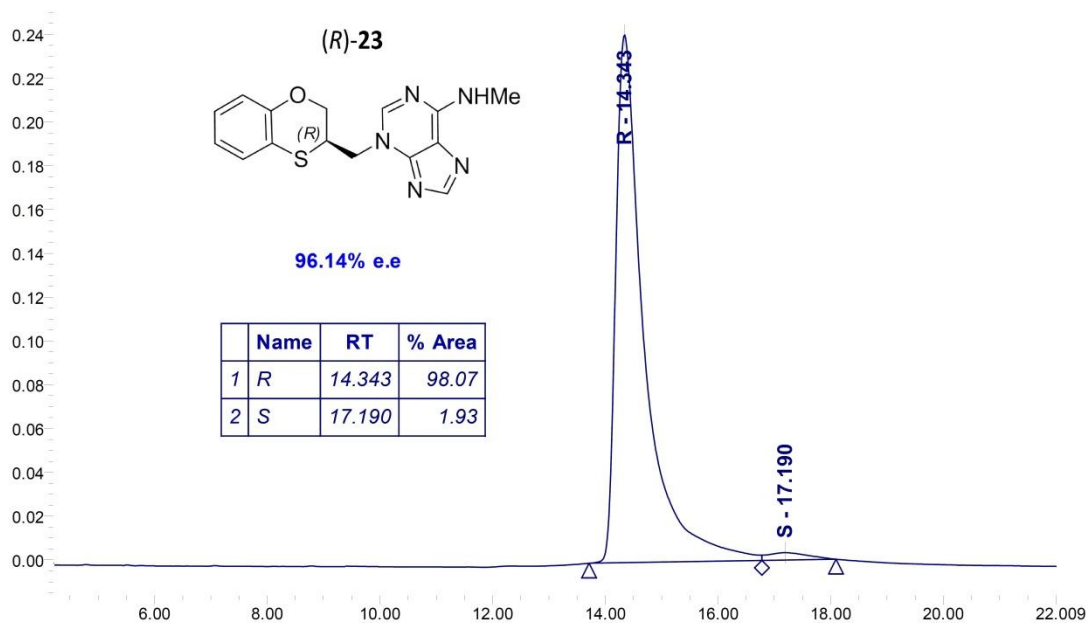


Figure S19

CHIRALPAK IA 250 x 4.6 mm
Flow rate: 1ml/min
room temperature
PDA 250.0 nm
n-hexane/ethanol 80/20 v/v

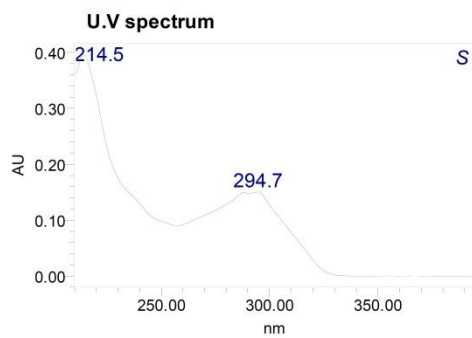
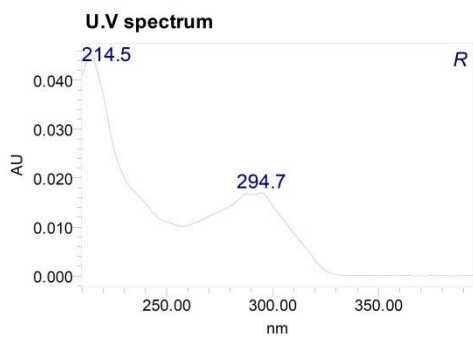
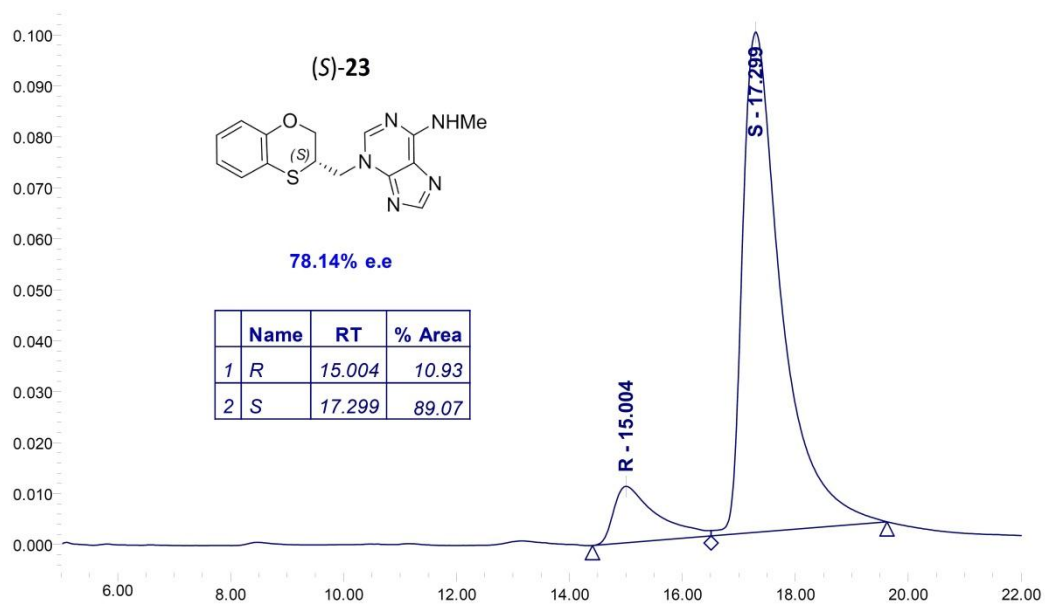


Figure S20

CHIRALPAK IA 250 x 4.6 mm
Flow rate: 1ml/min
room temperature
PDA 250.0 nm
n-hexane/ethanol 80/20 v/v

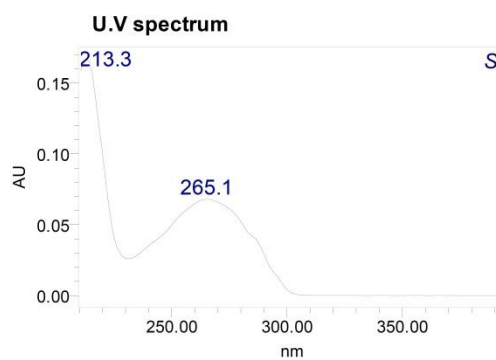
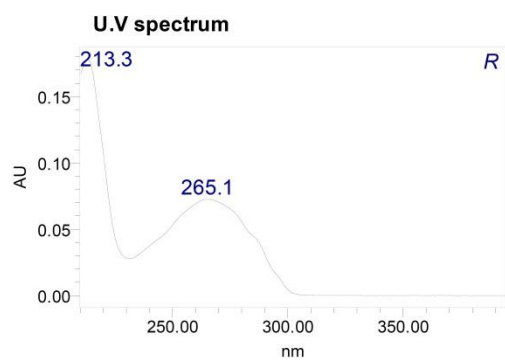
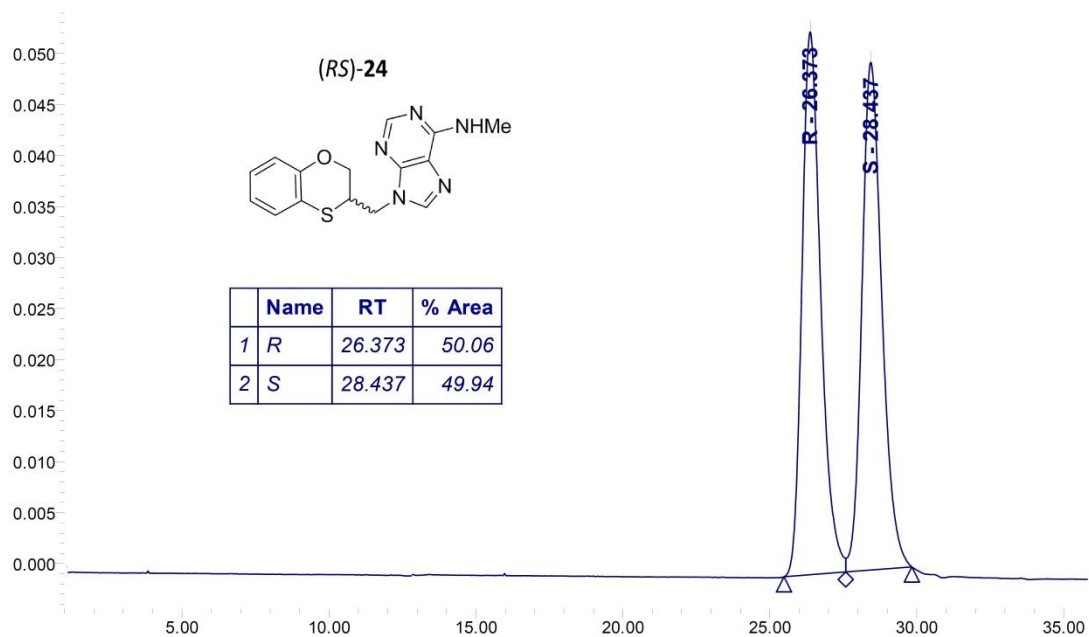


Figure S21

CHIRALPAK IA 250 x 4.6 mm
Flow rate: 1ml/min
room temperature
PDA 250.0 nm
n-hexane/ethanol 80/20 v/v

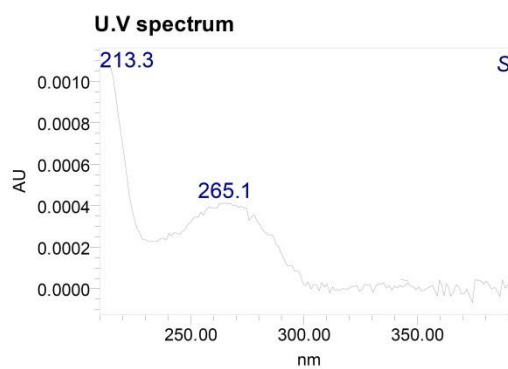
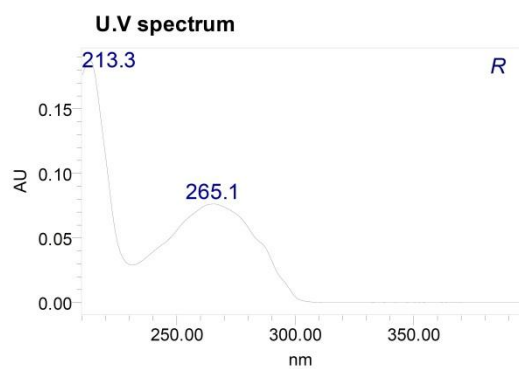
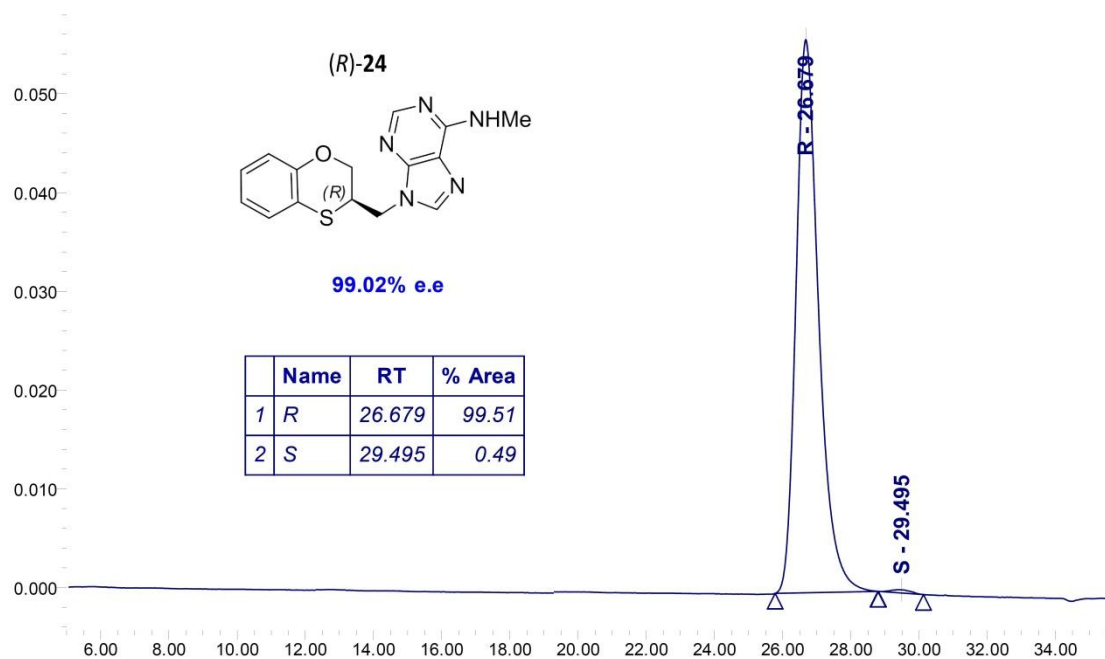


Figure S22

CHIRALPAK IA 250 x 4.6 mm
Flow rate: 1ml/min
room temperature
PDA 250.0 nm
n-hexane/ethanol 80/20 v/v

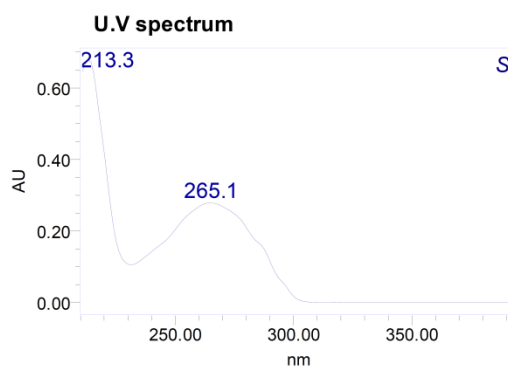
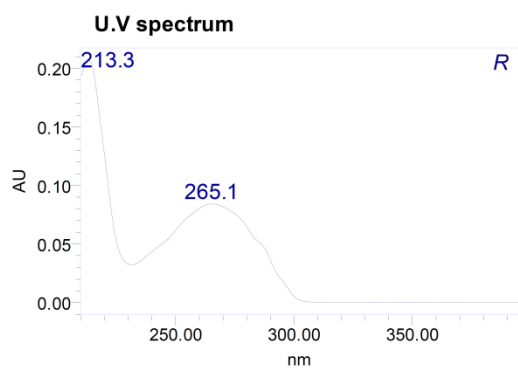
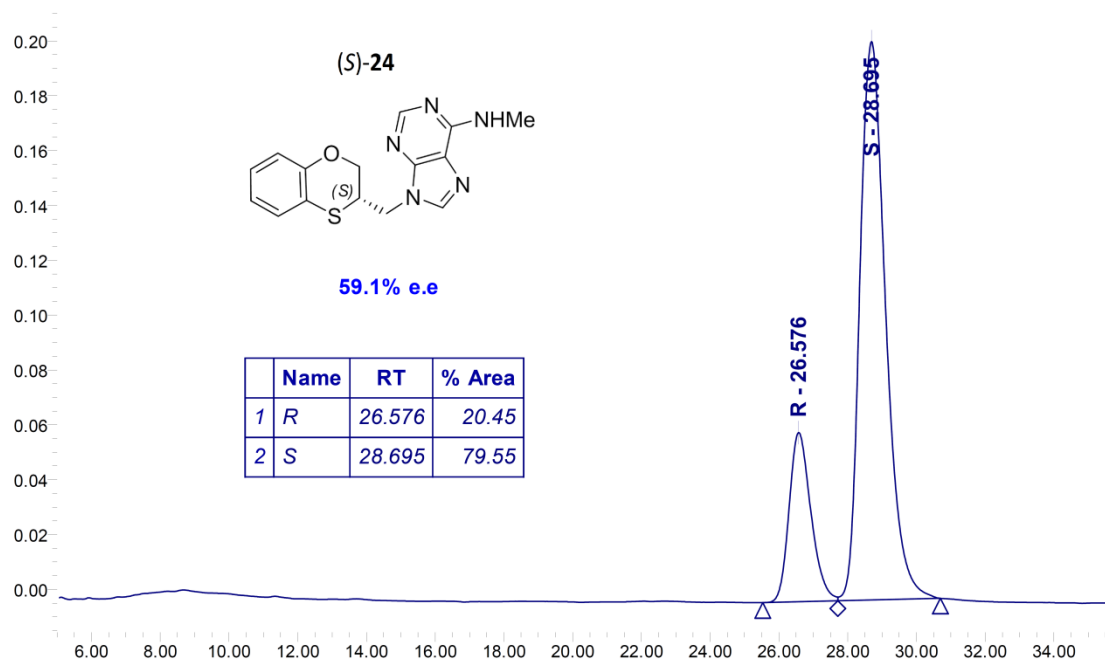
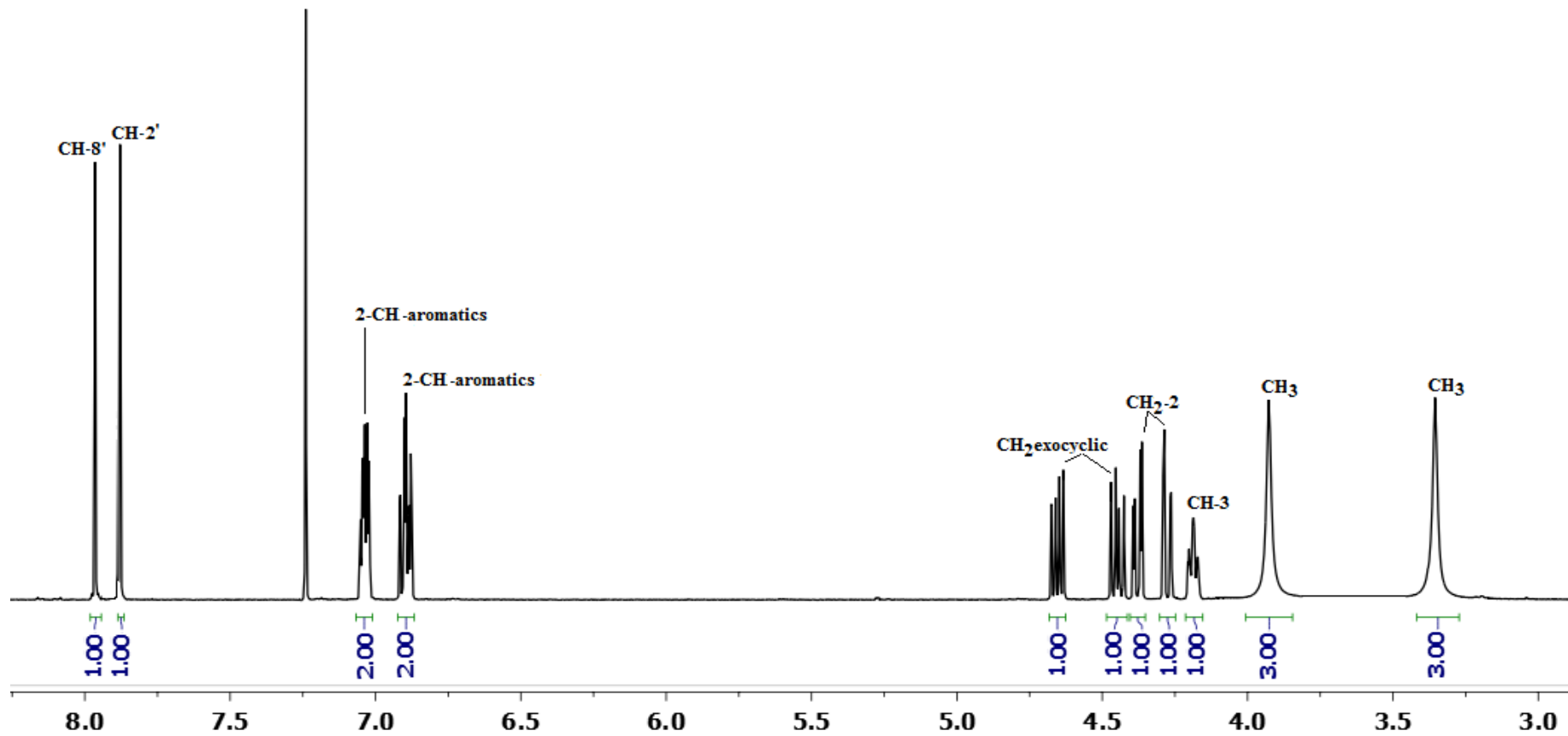
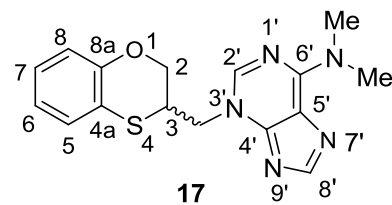


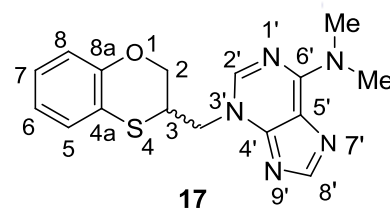
Figure S23

500 MHz, CDCl₃

500 MHz, CDCl₃

153.85
152.74
151.27
150.11
— 141.92

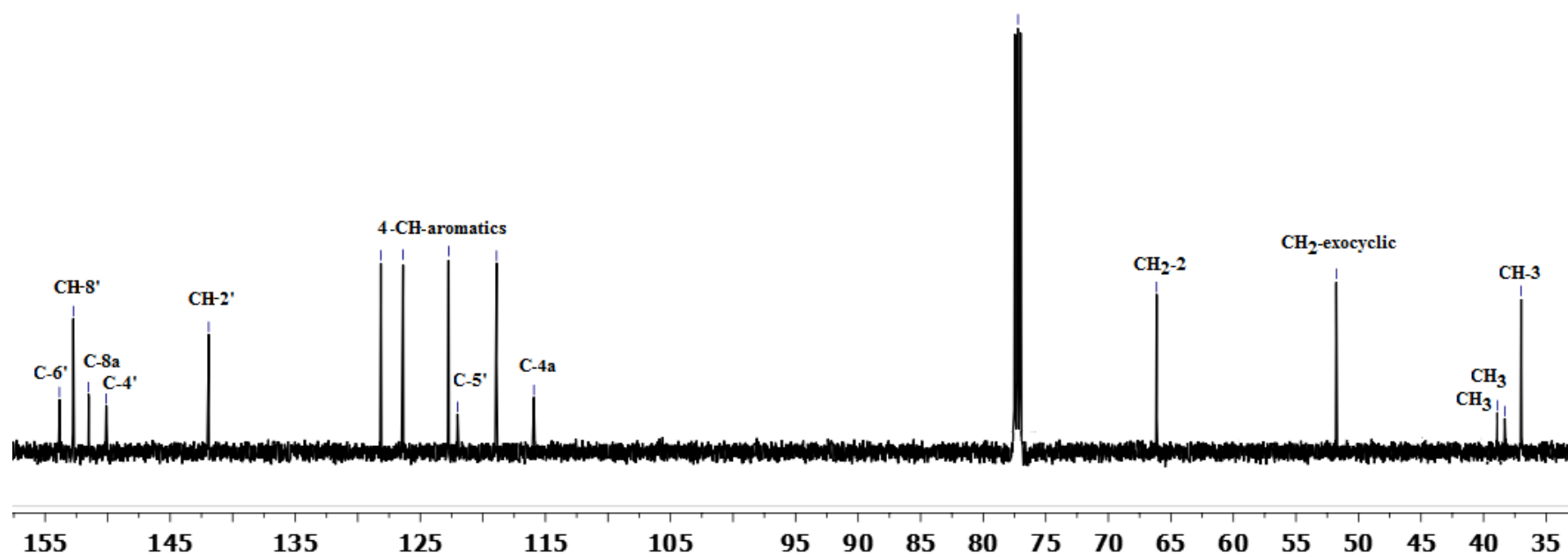
128.15
126.38
122.74
122.02
118.91
115.92



— 66.14

— 51.77

39.95
38.23
— 36.99



500 MHz, CDCl₃

— 152.74

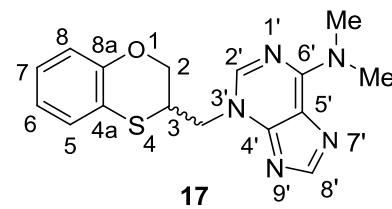
— 141.92

— 128.15

— 126.38

— 122.74

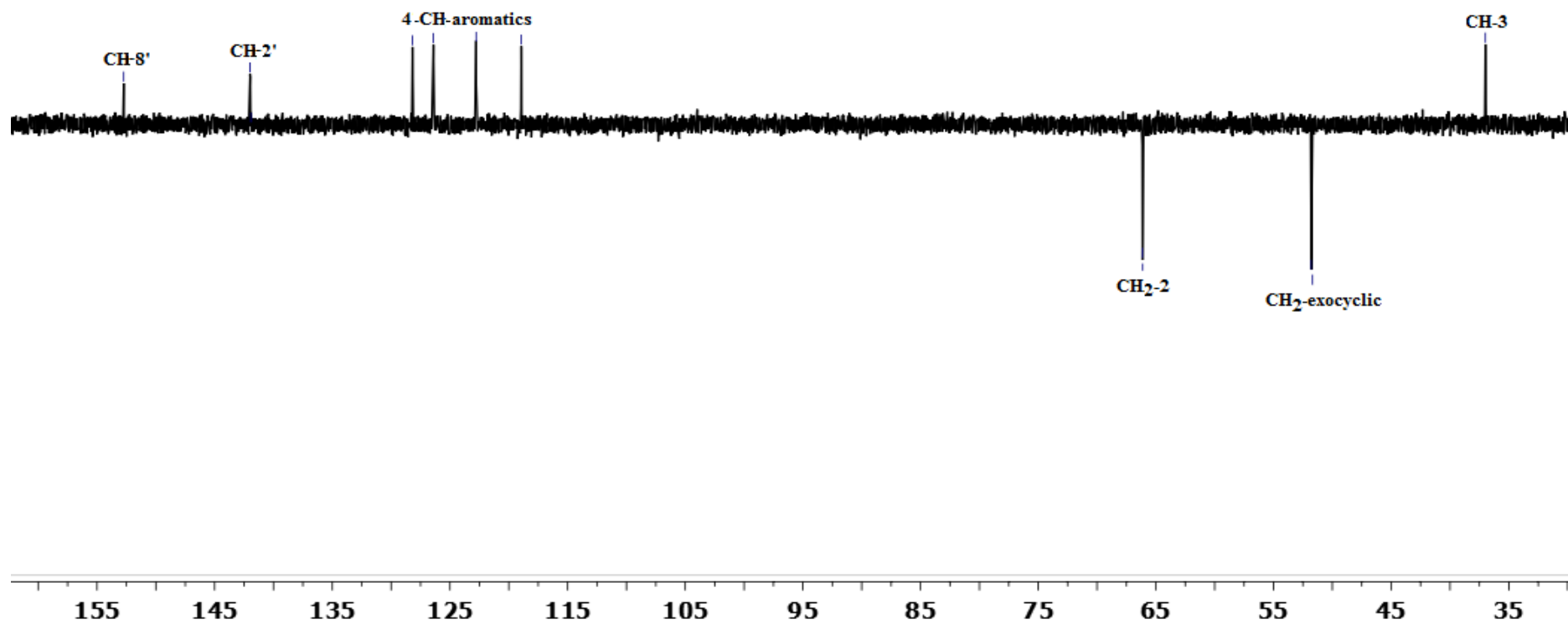
— 118.91

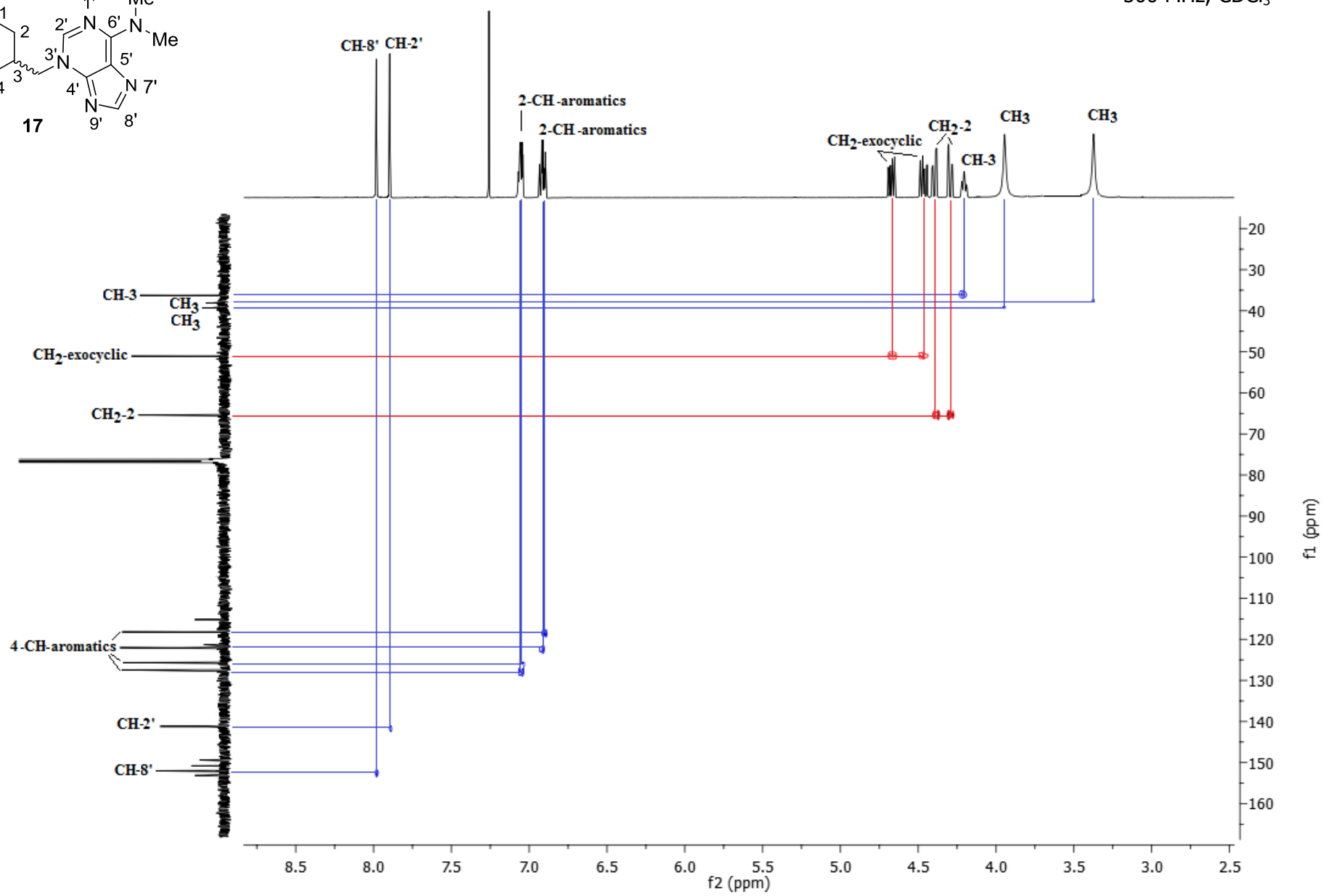
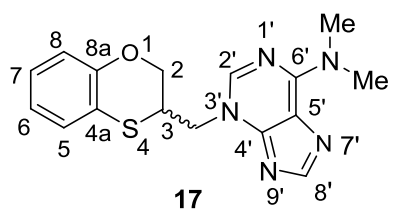


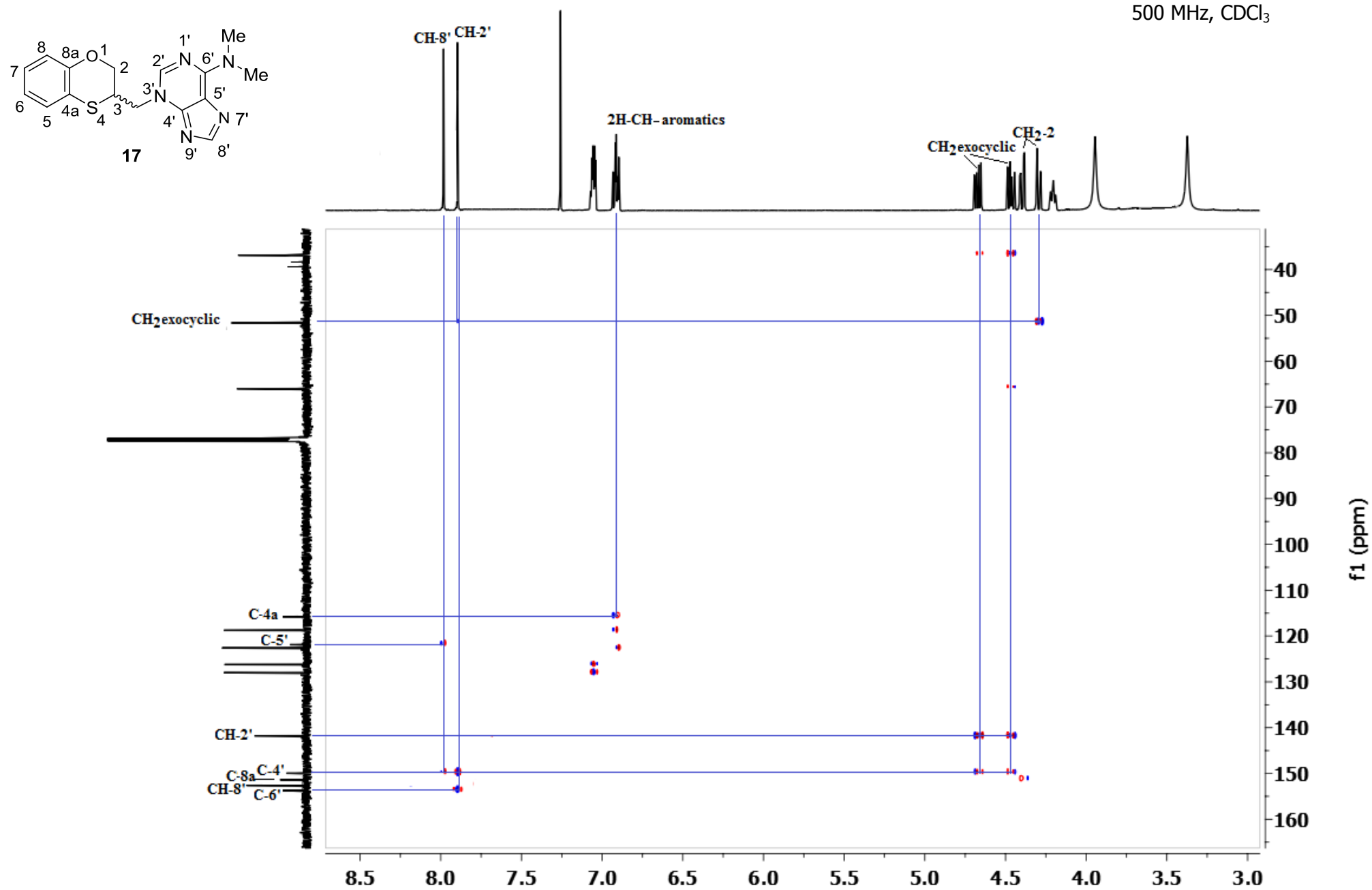
— 66.14

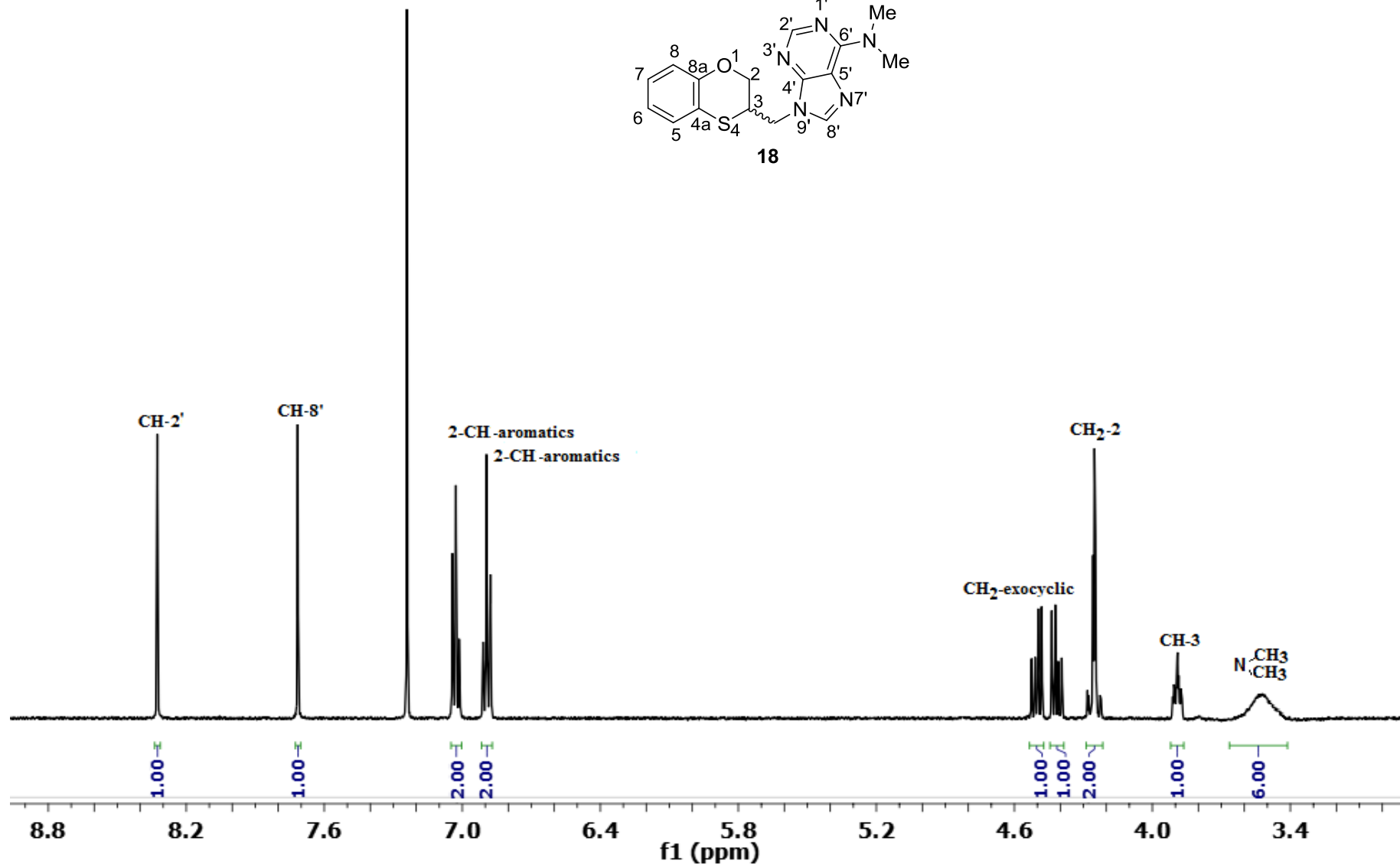
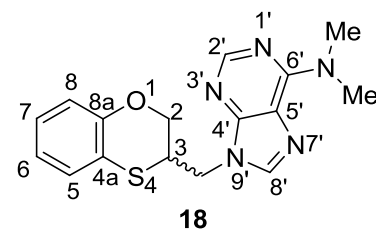
— 51.77

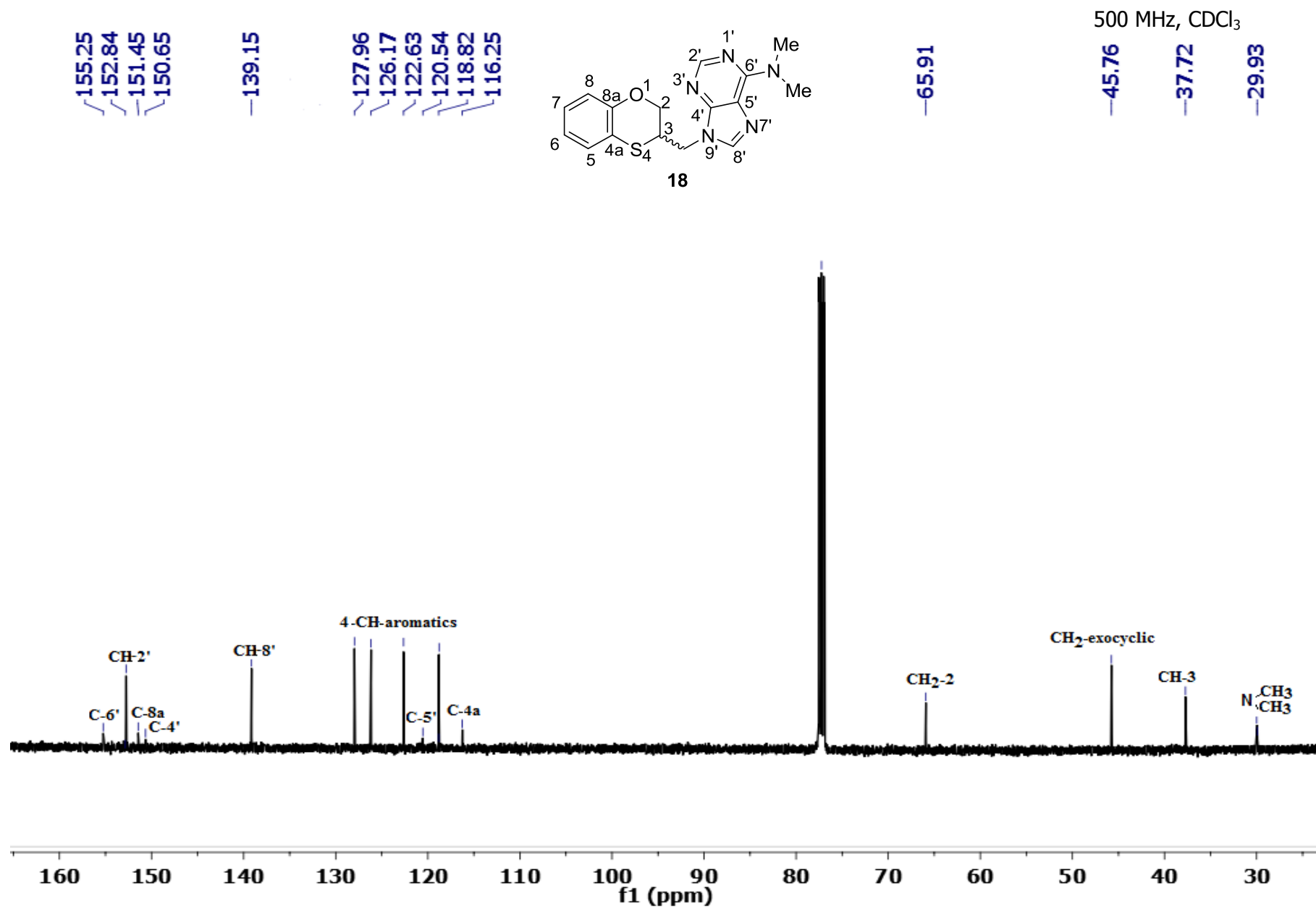
— 36.99



500 MHz, CDCl₃







500 MHz, CDCl₃

—152.84

—139.15

~127.96

~126.17

~122.63

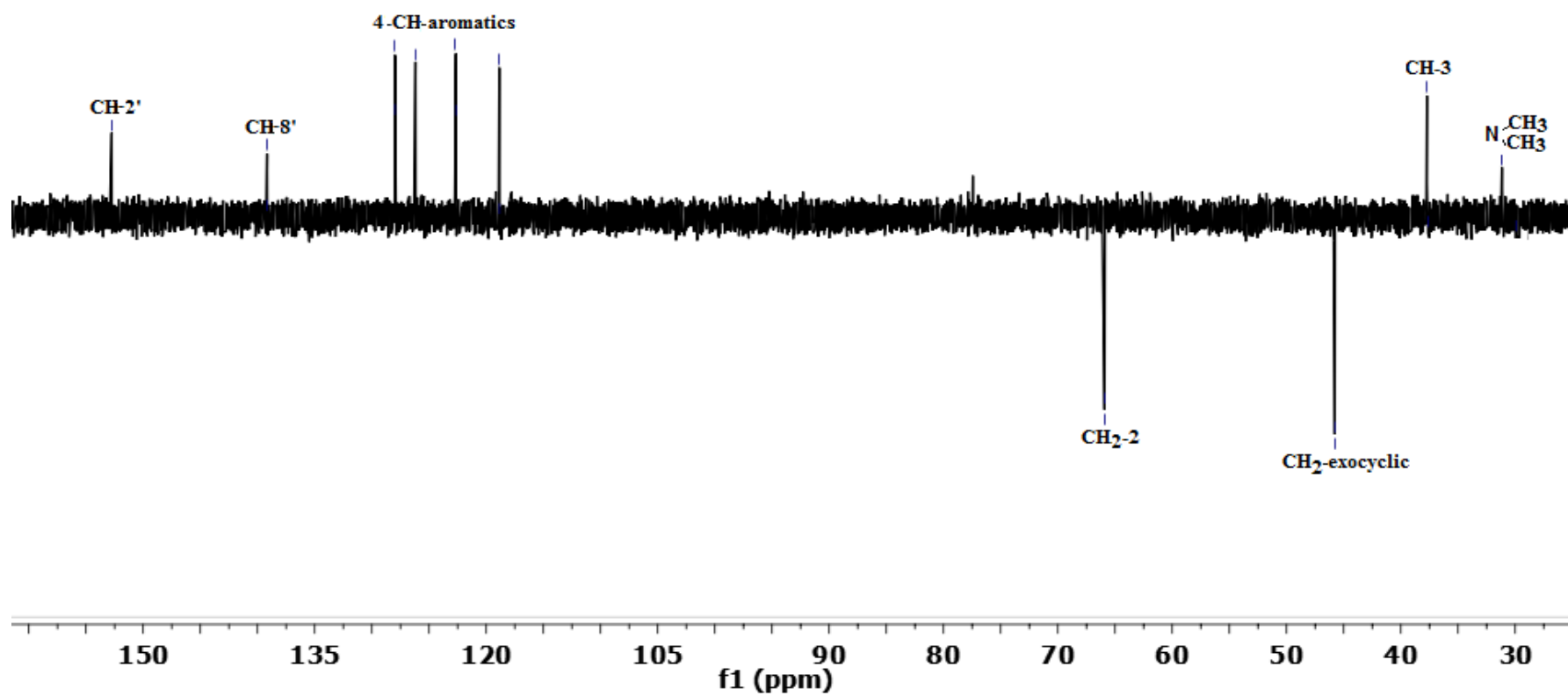
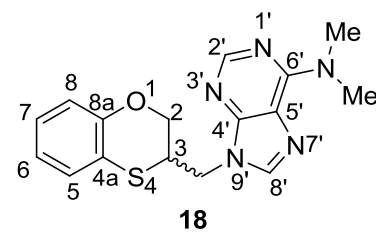
~118.82

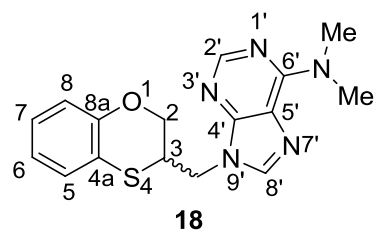
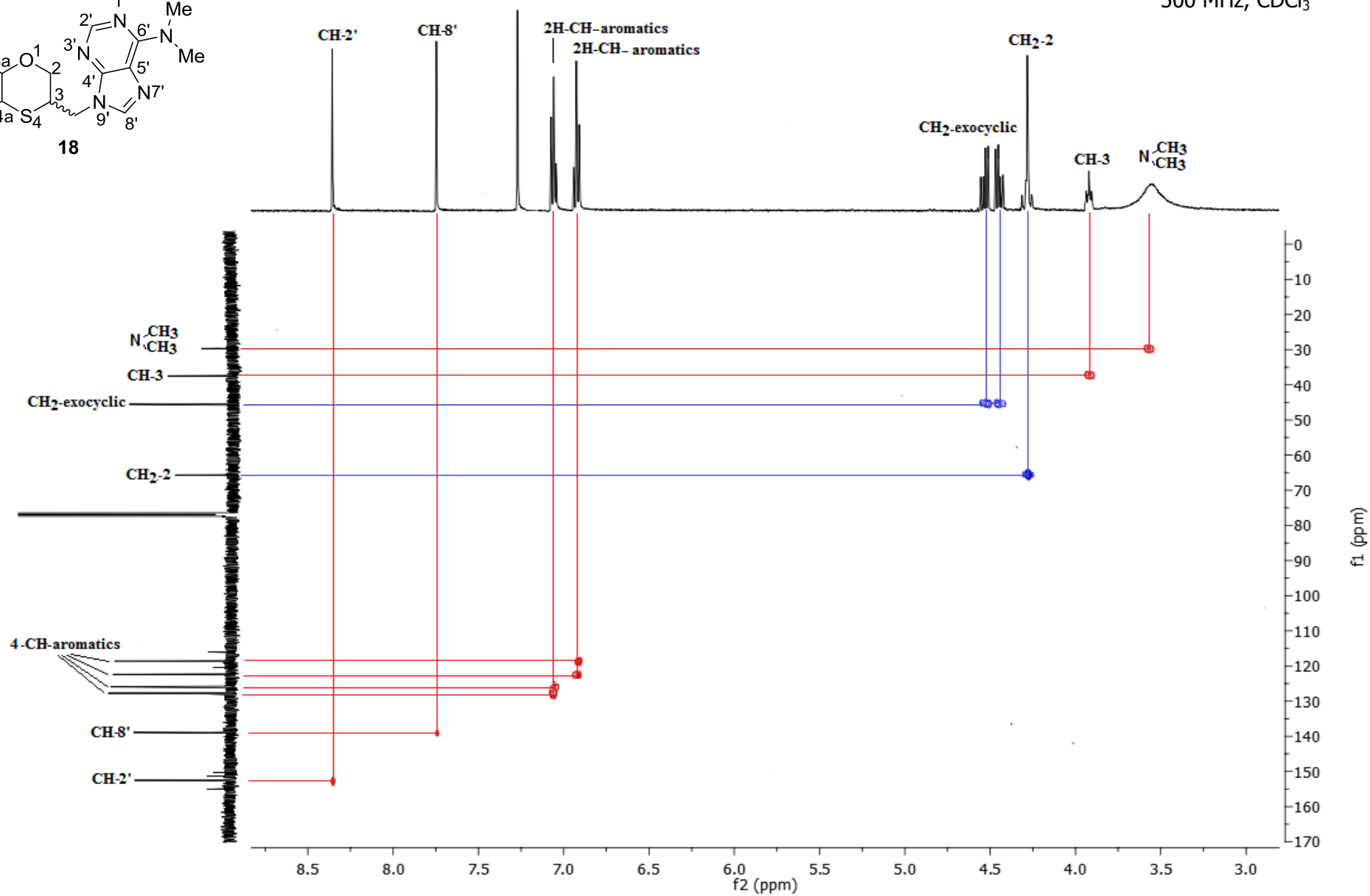
—65.91

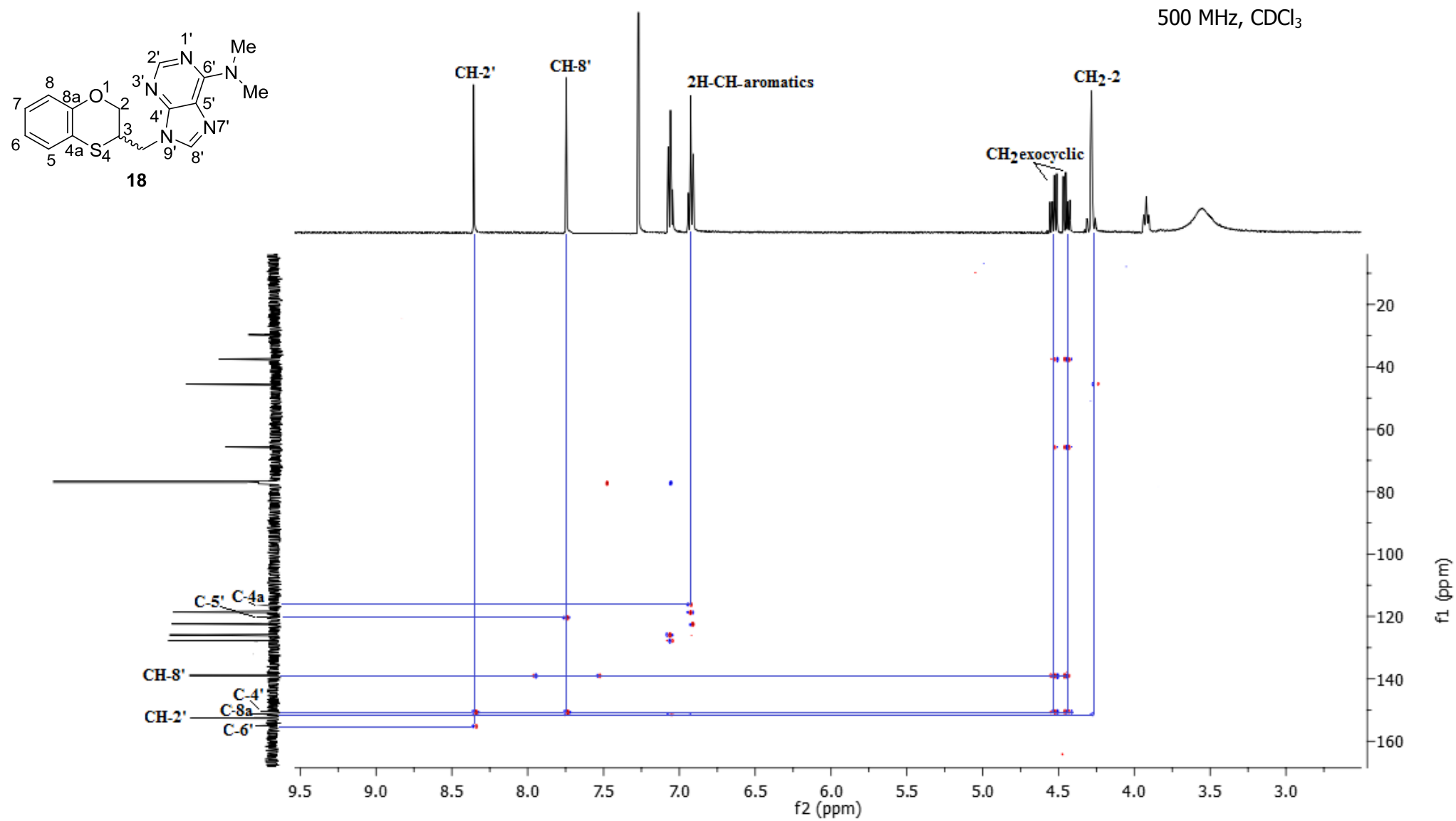
—45.76

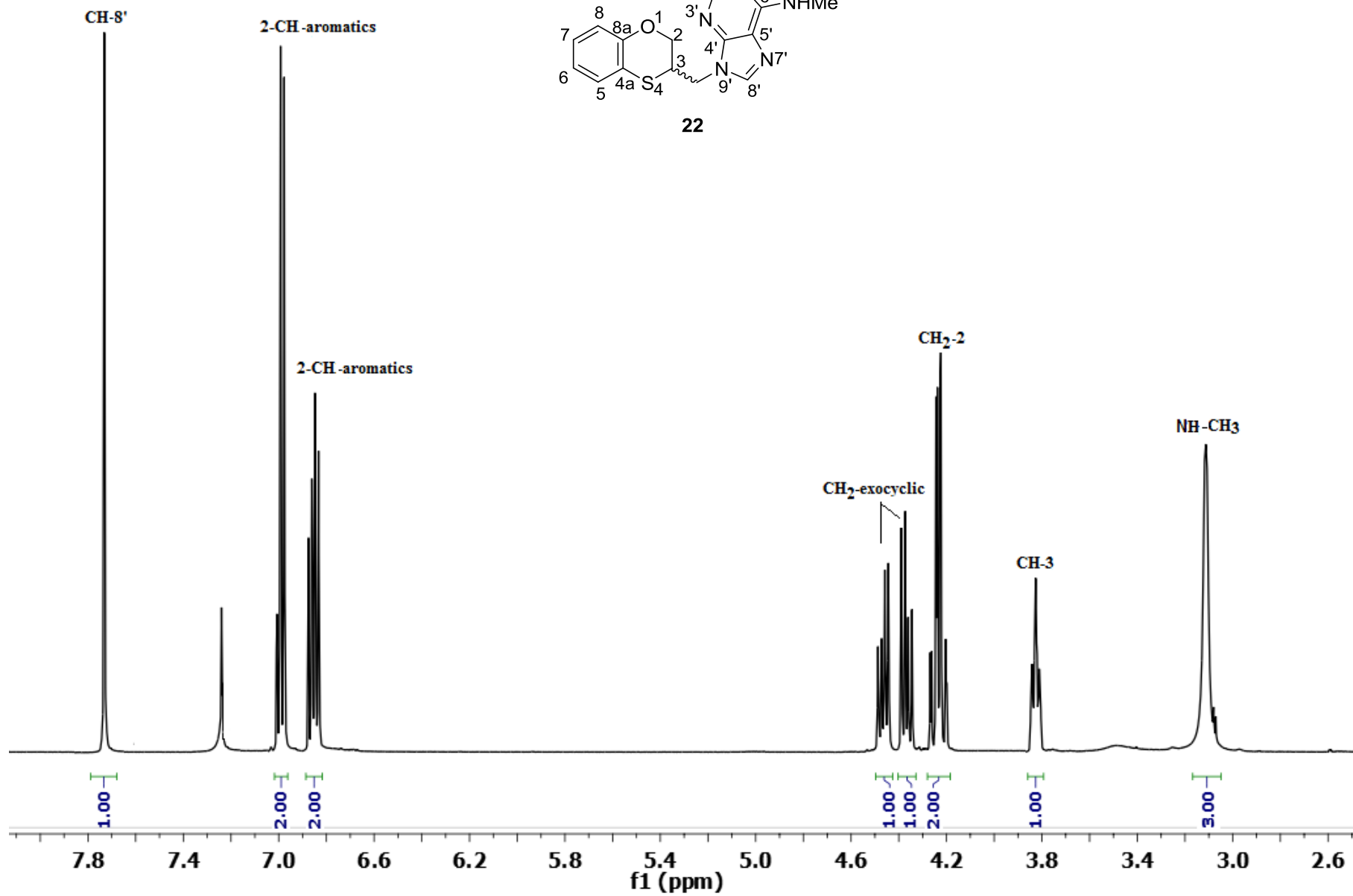
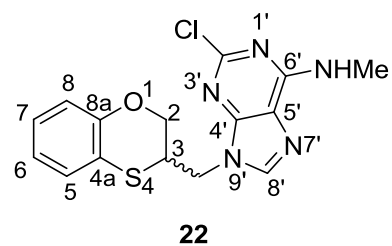
—37.72

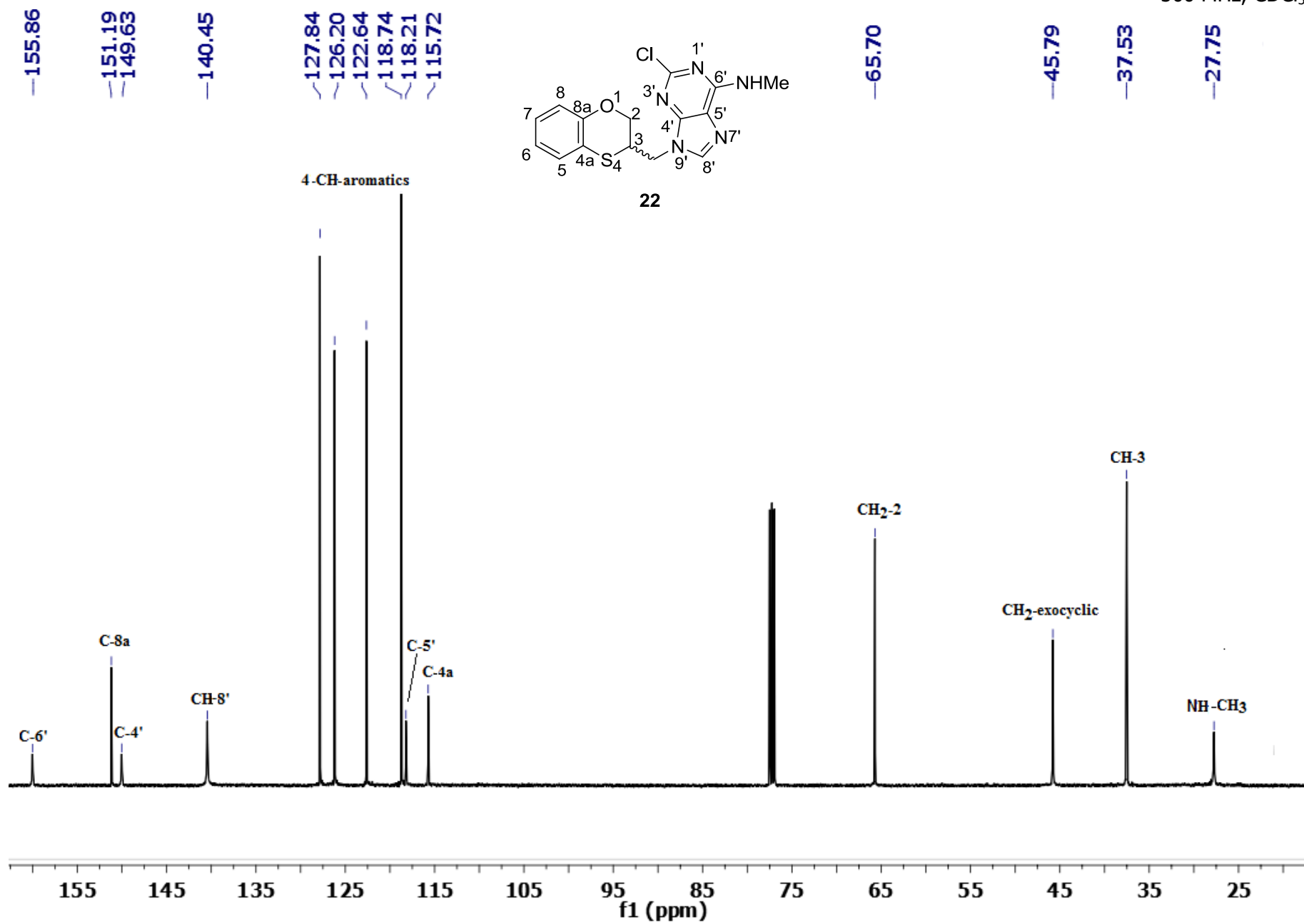
—29.93

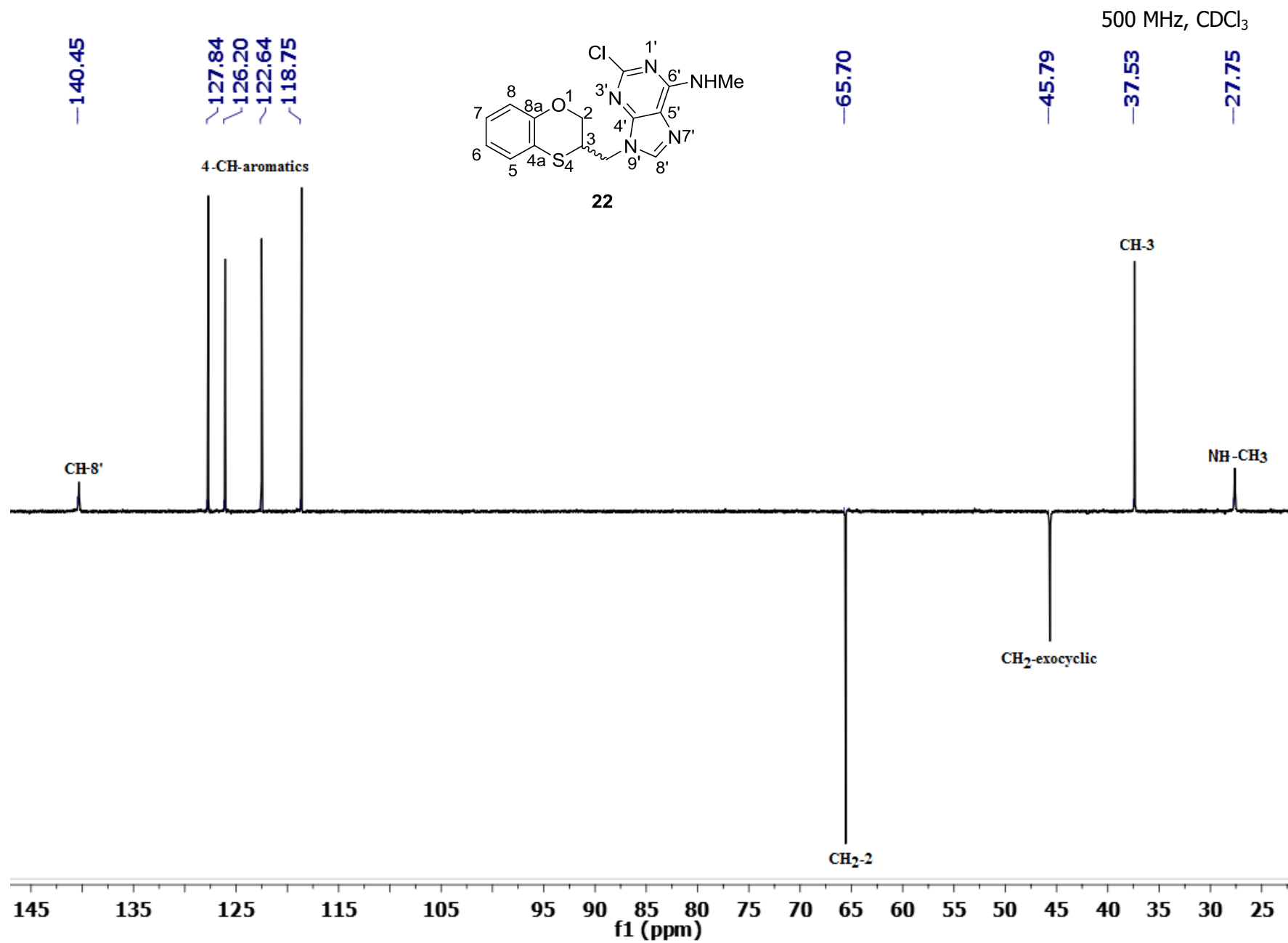


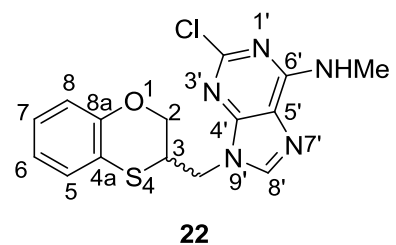
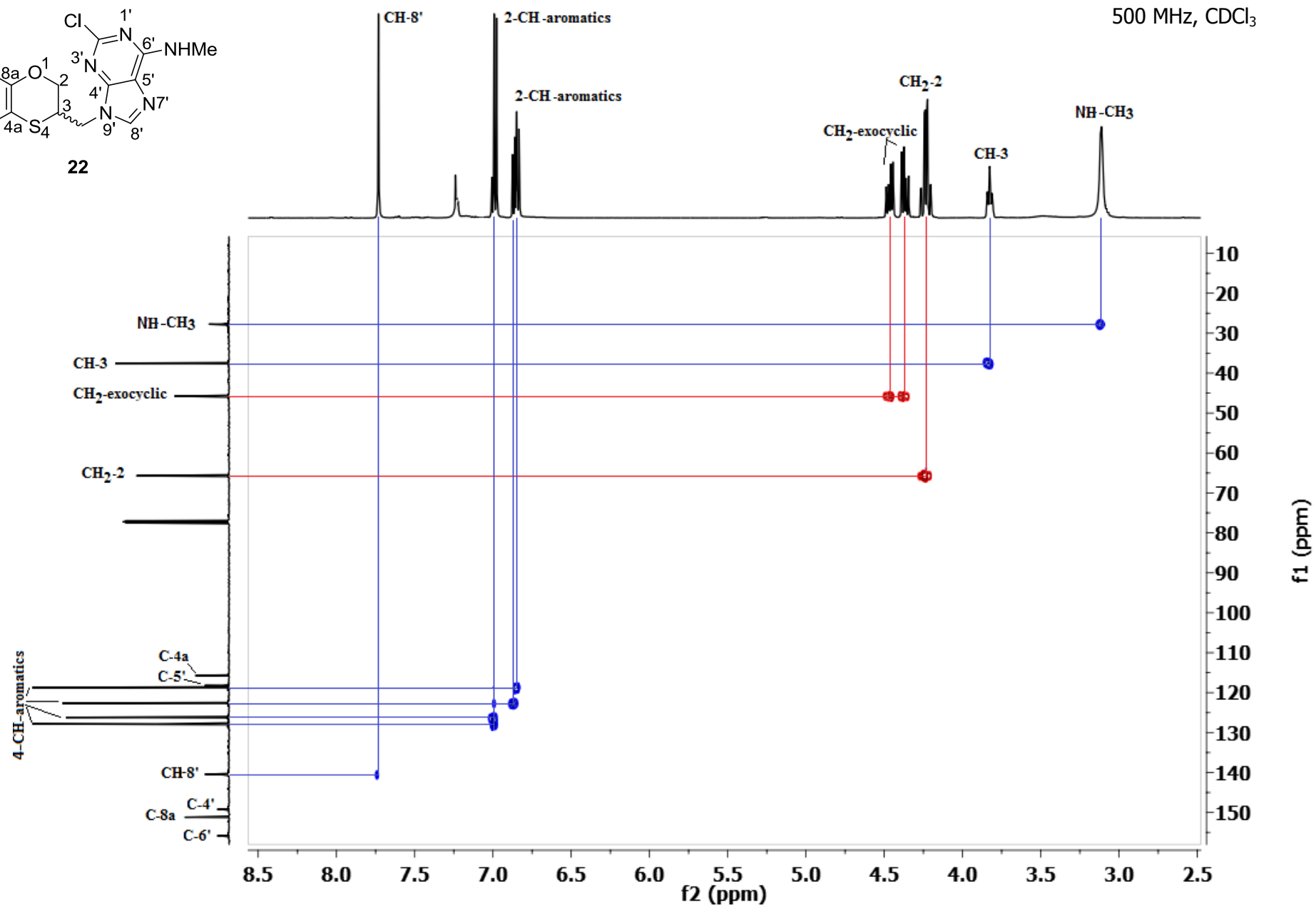
500 MHz, CDCl₃

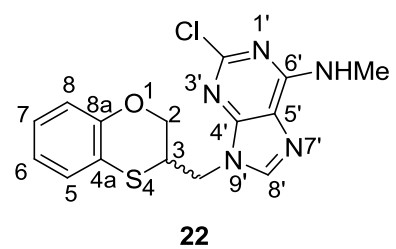
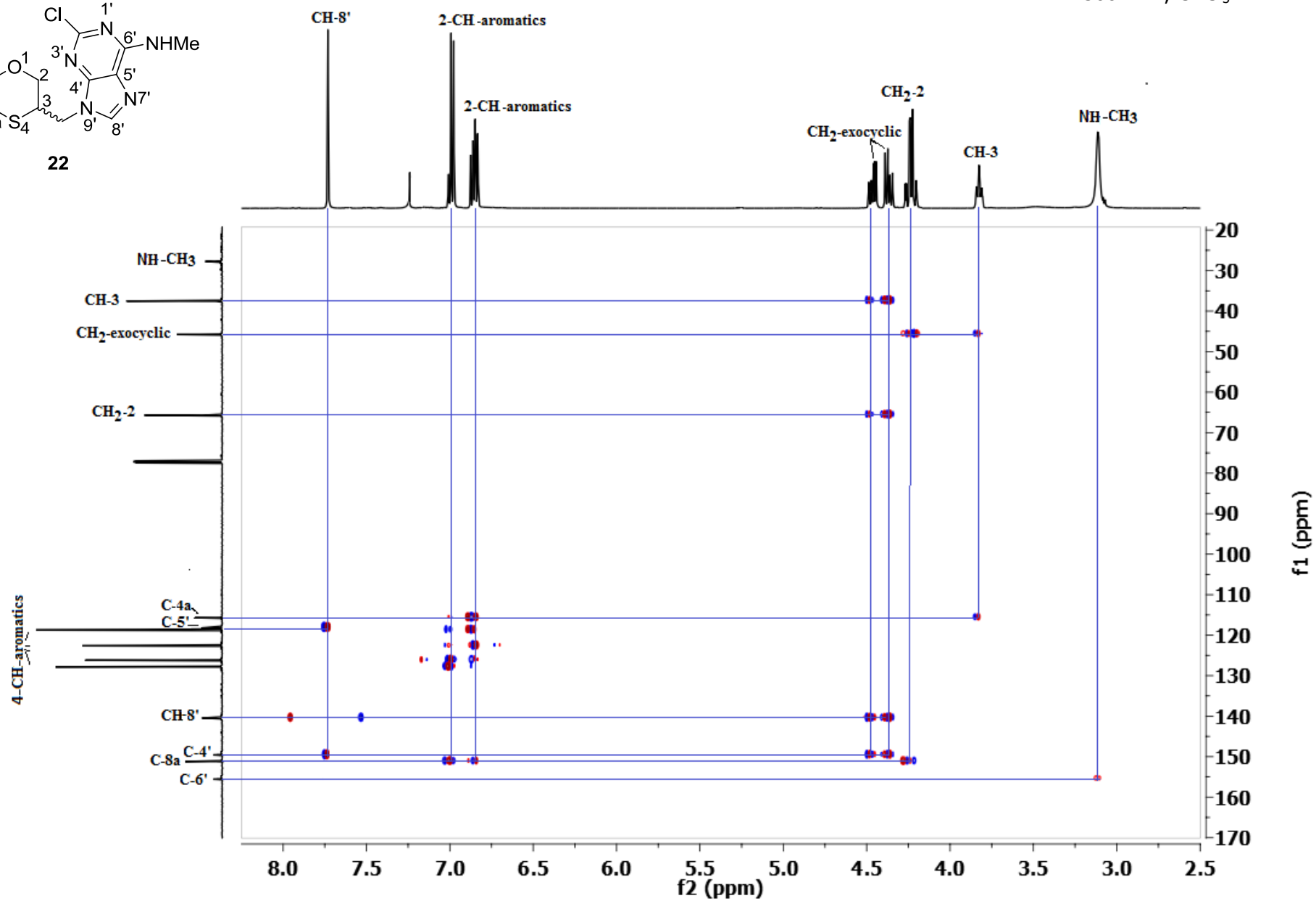


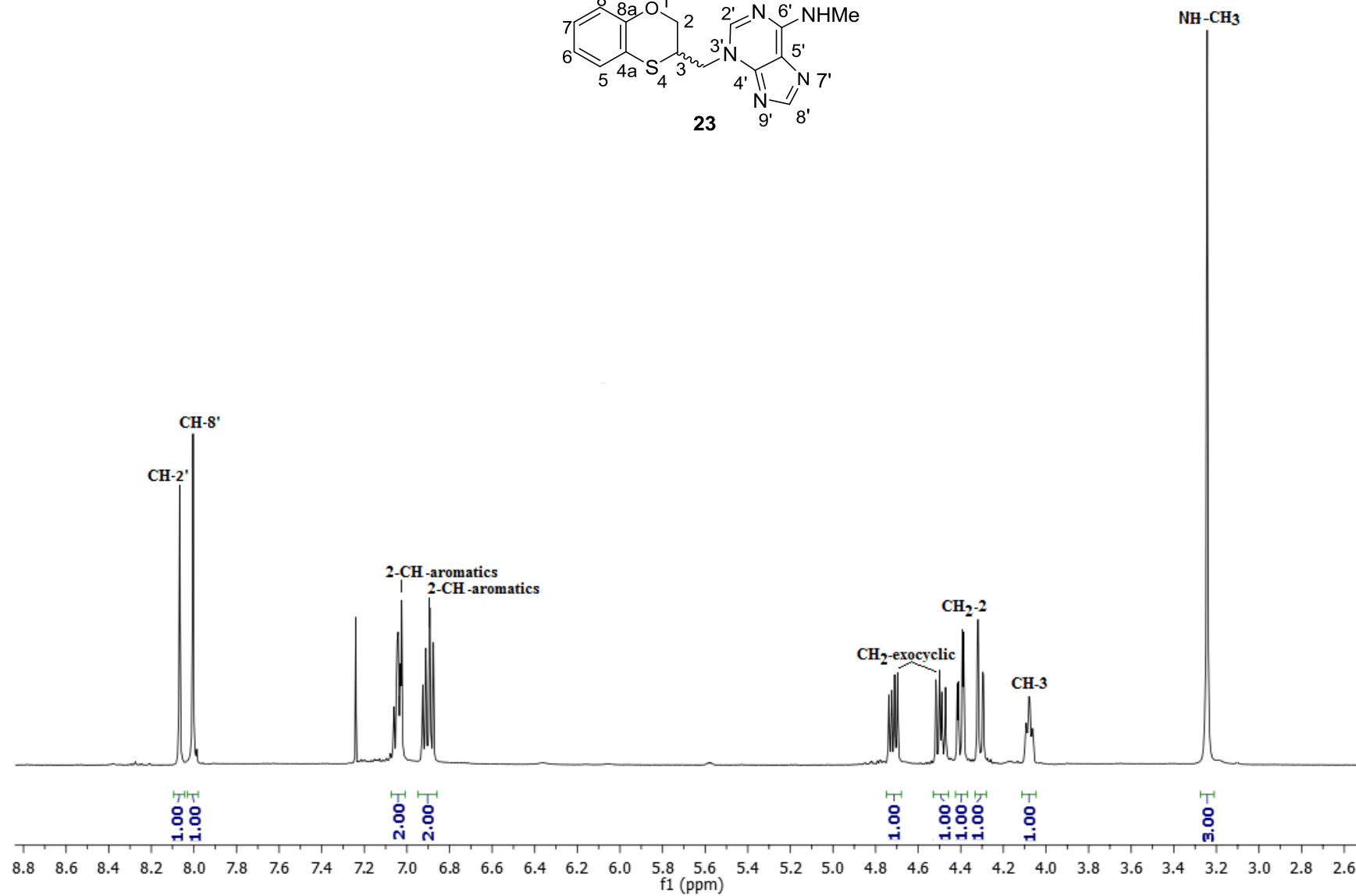
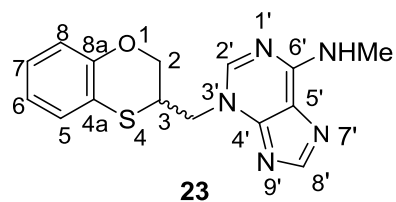
500 MHz, CDCl₃

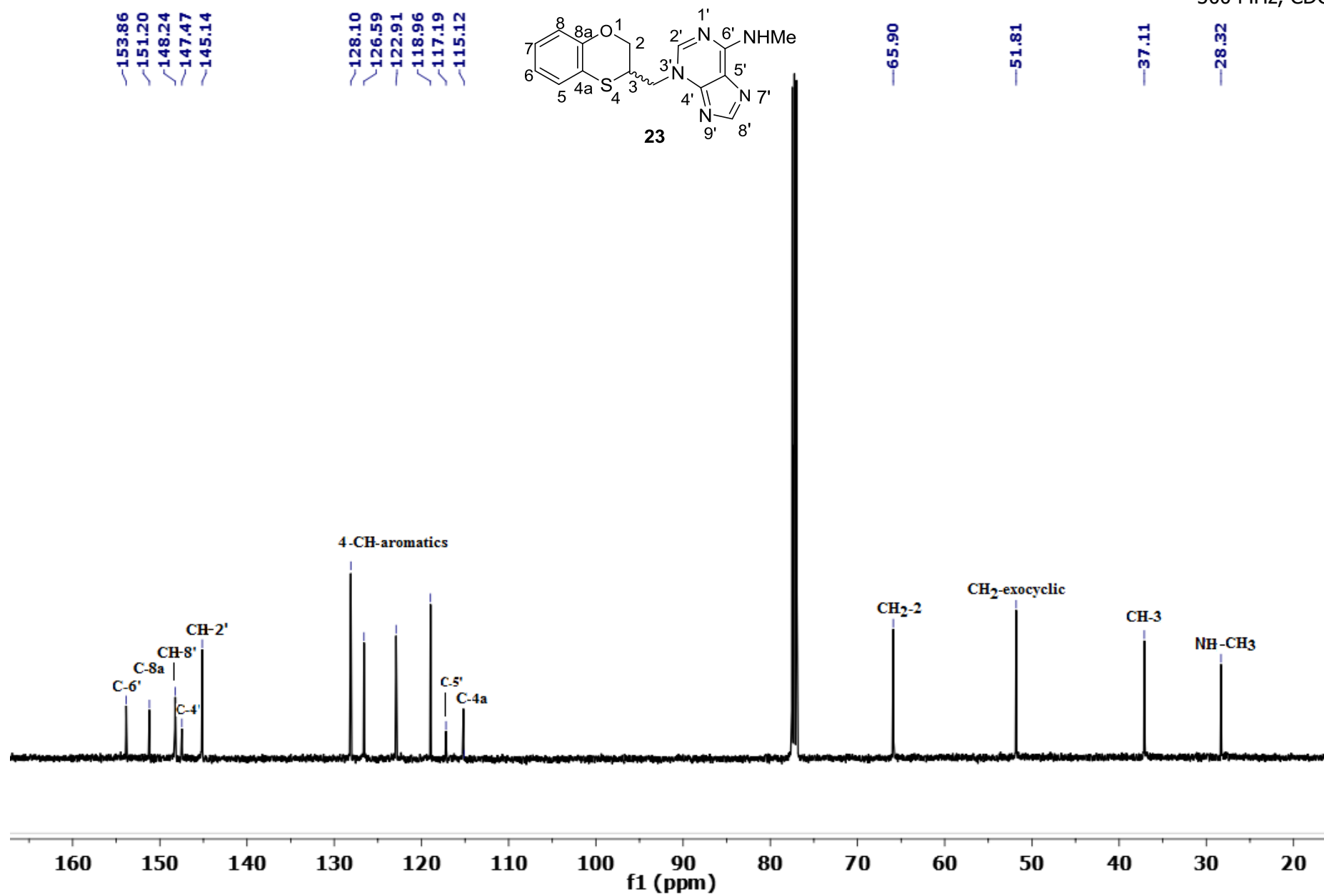
500 MHz, CDCl₃

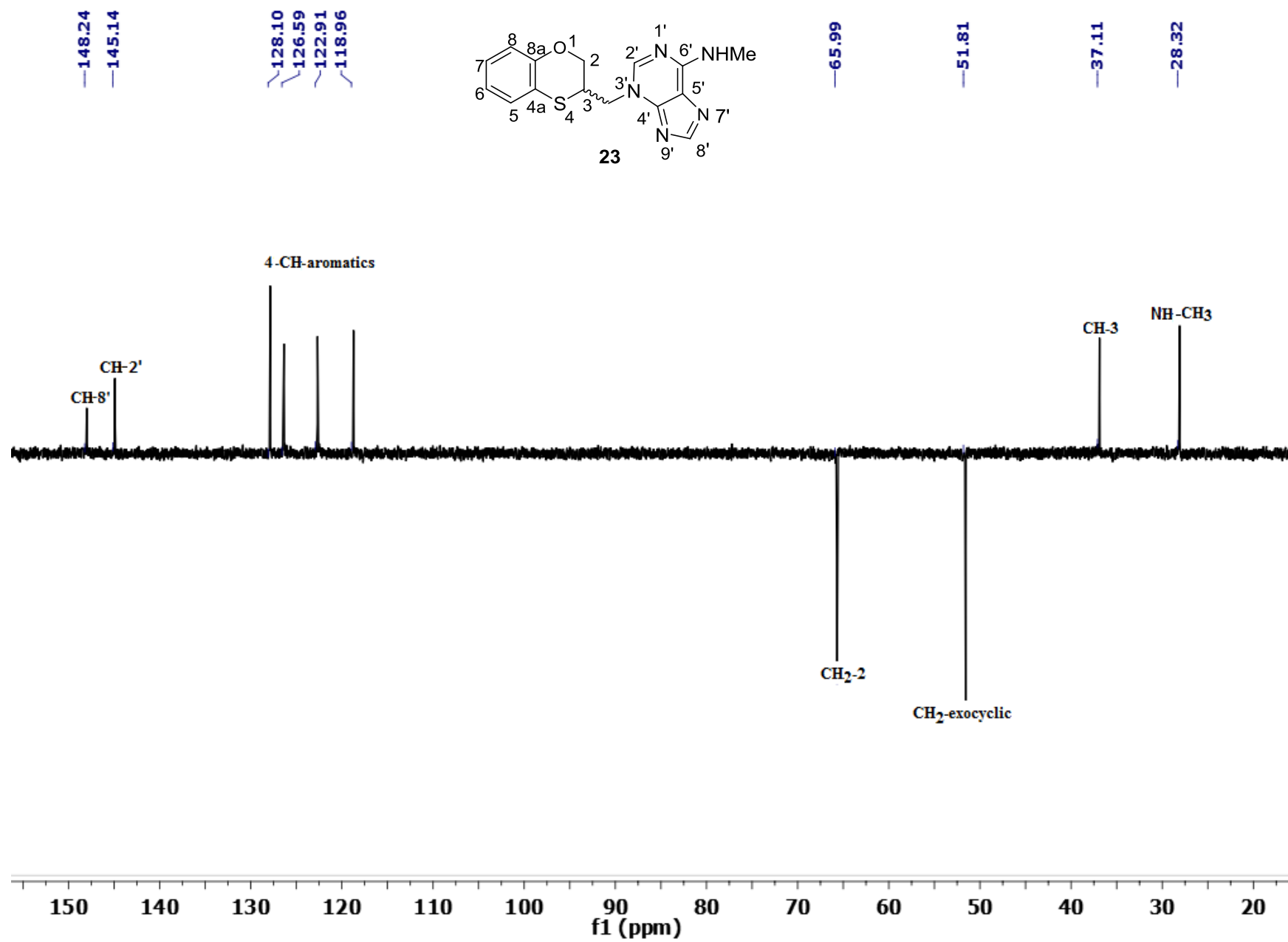


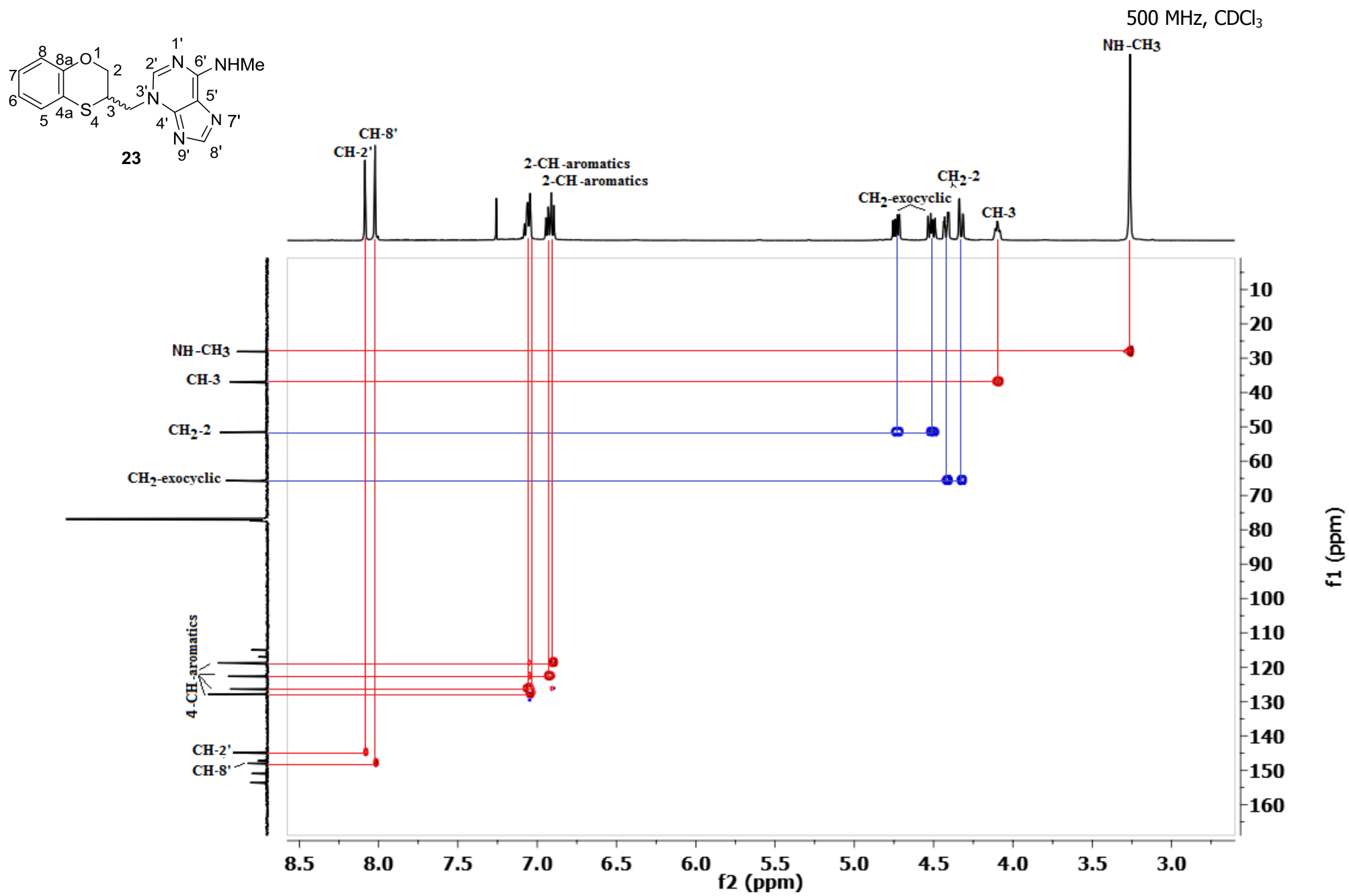
500 MHz, CDCl₃

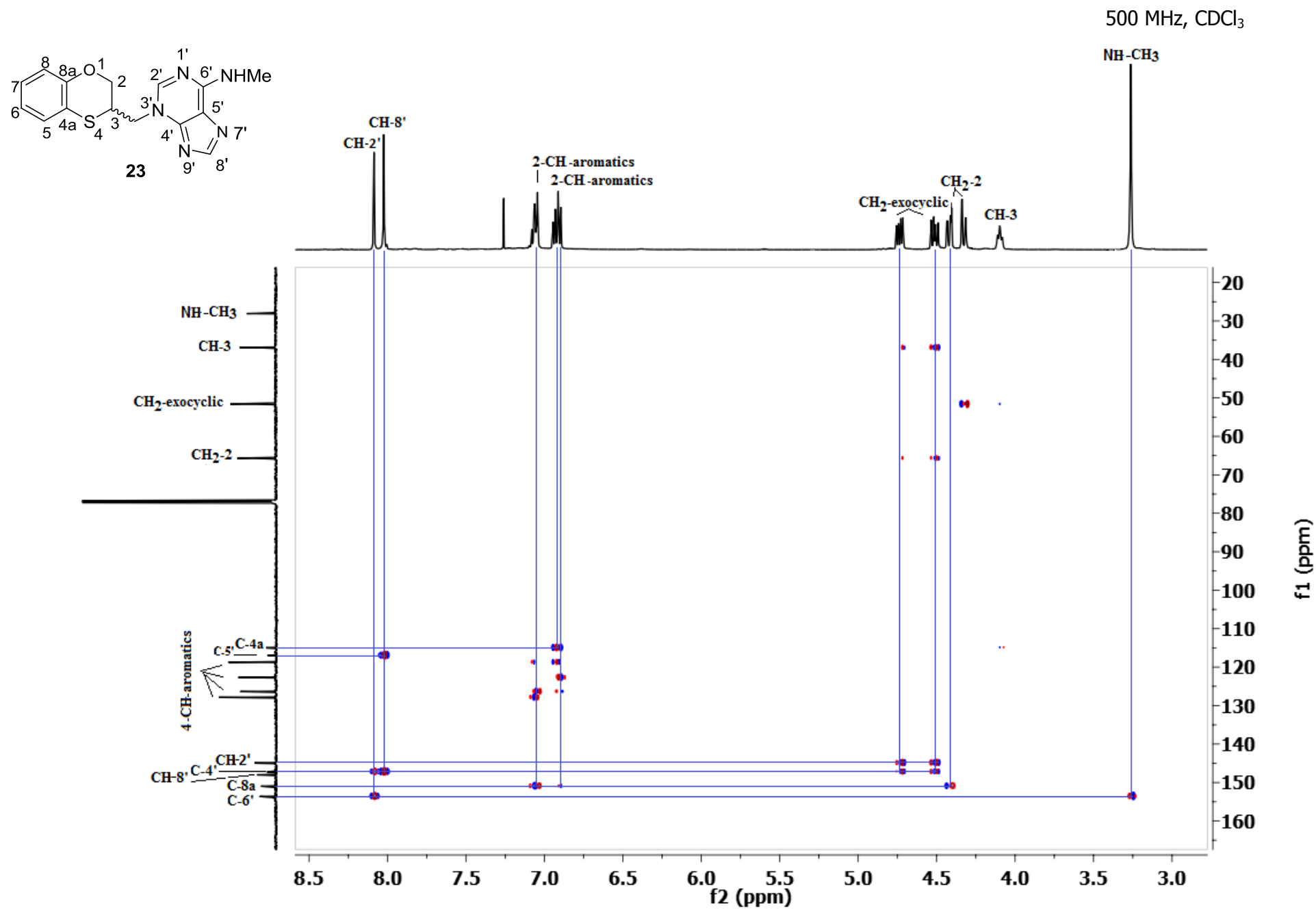
500 MHz, CDCl₃

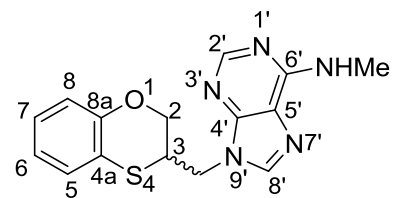
500 MHz, CDCl₃

500 MHz, CDCl₃

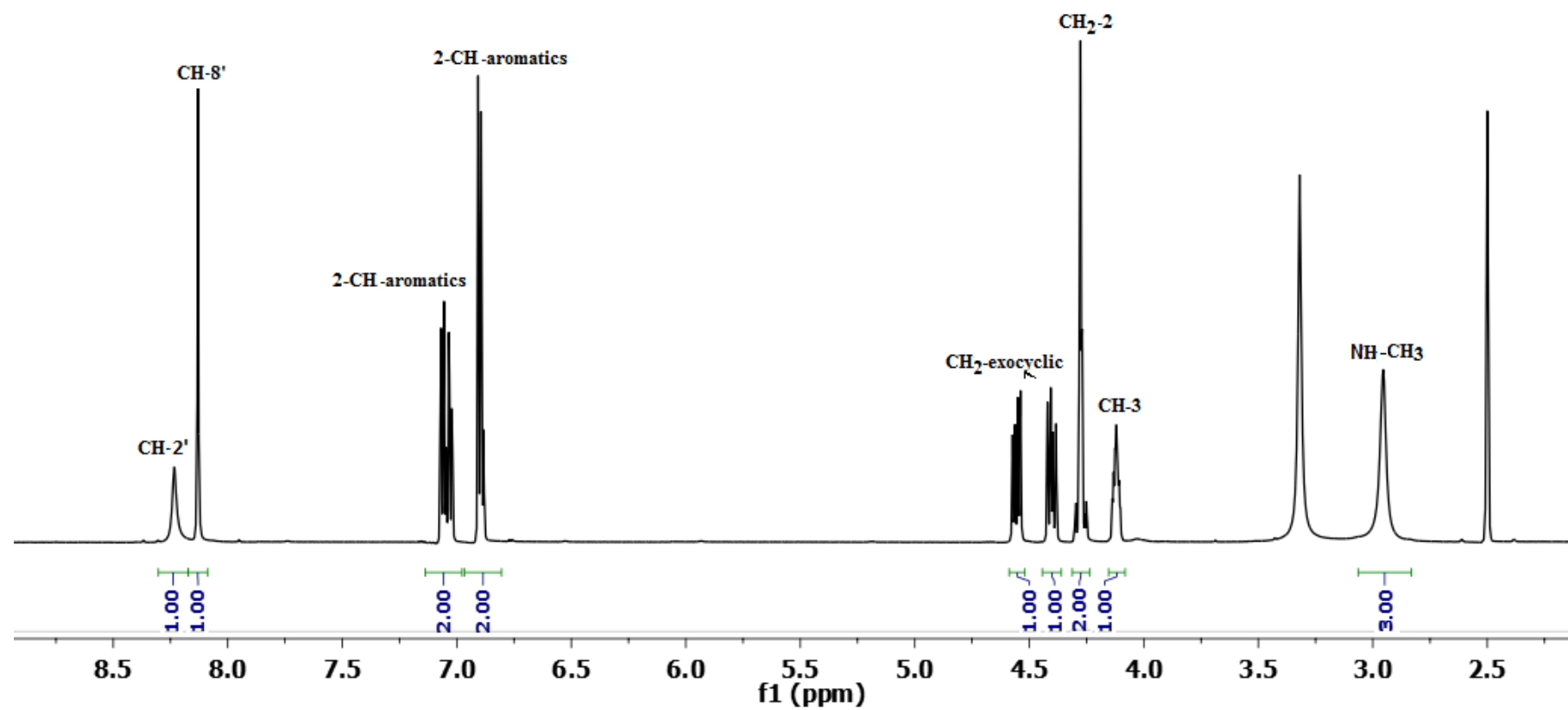
500 MHz, CDCl₃

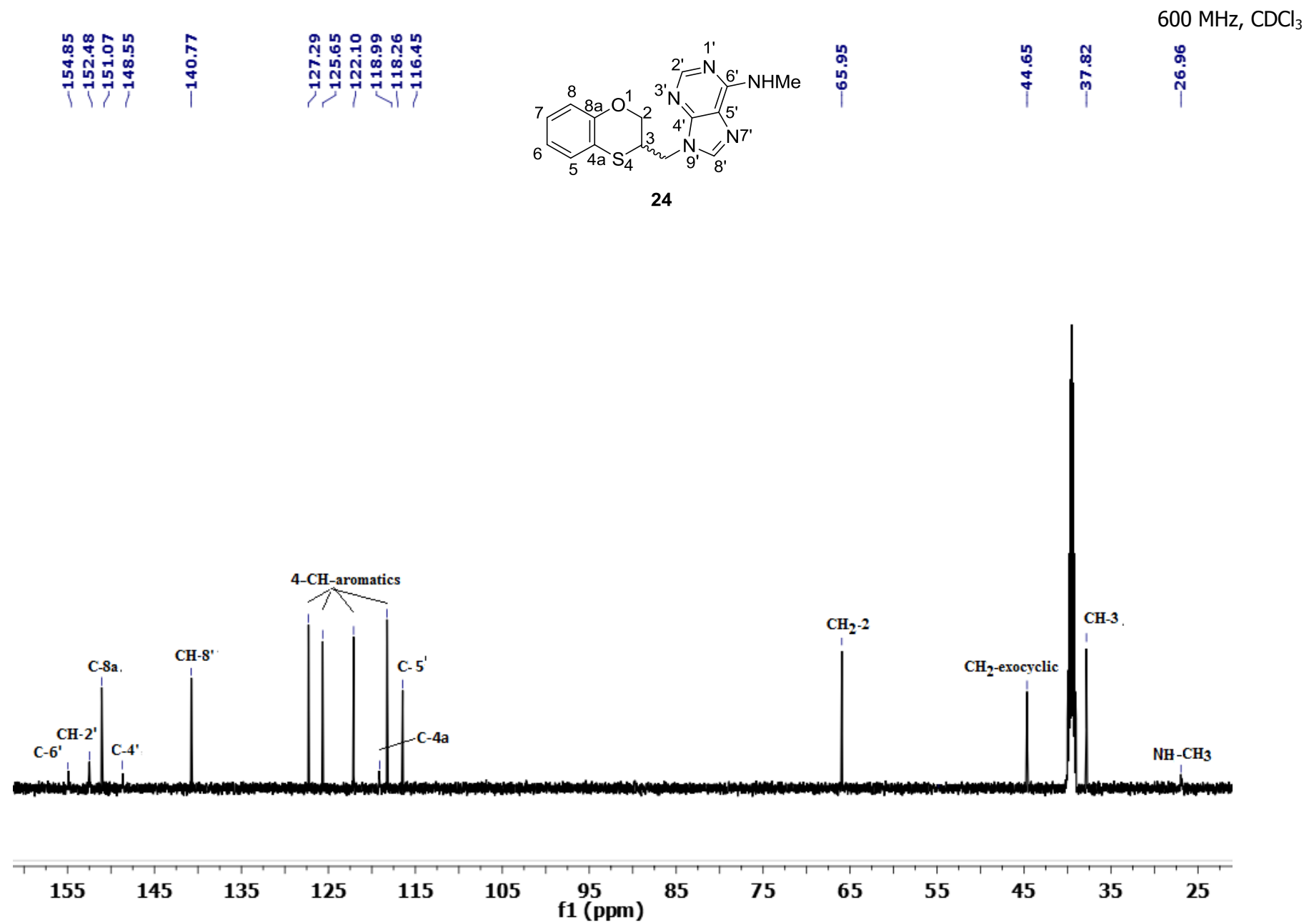


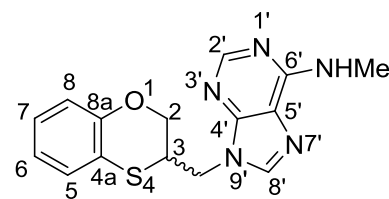




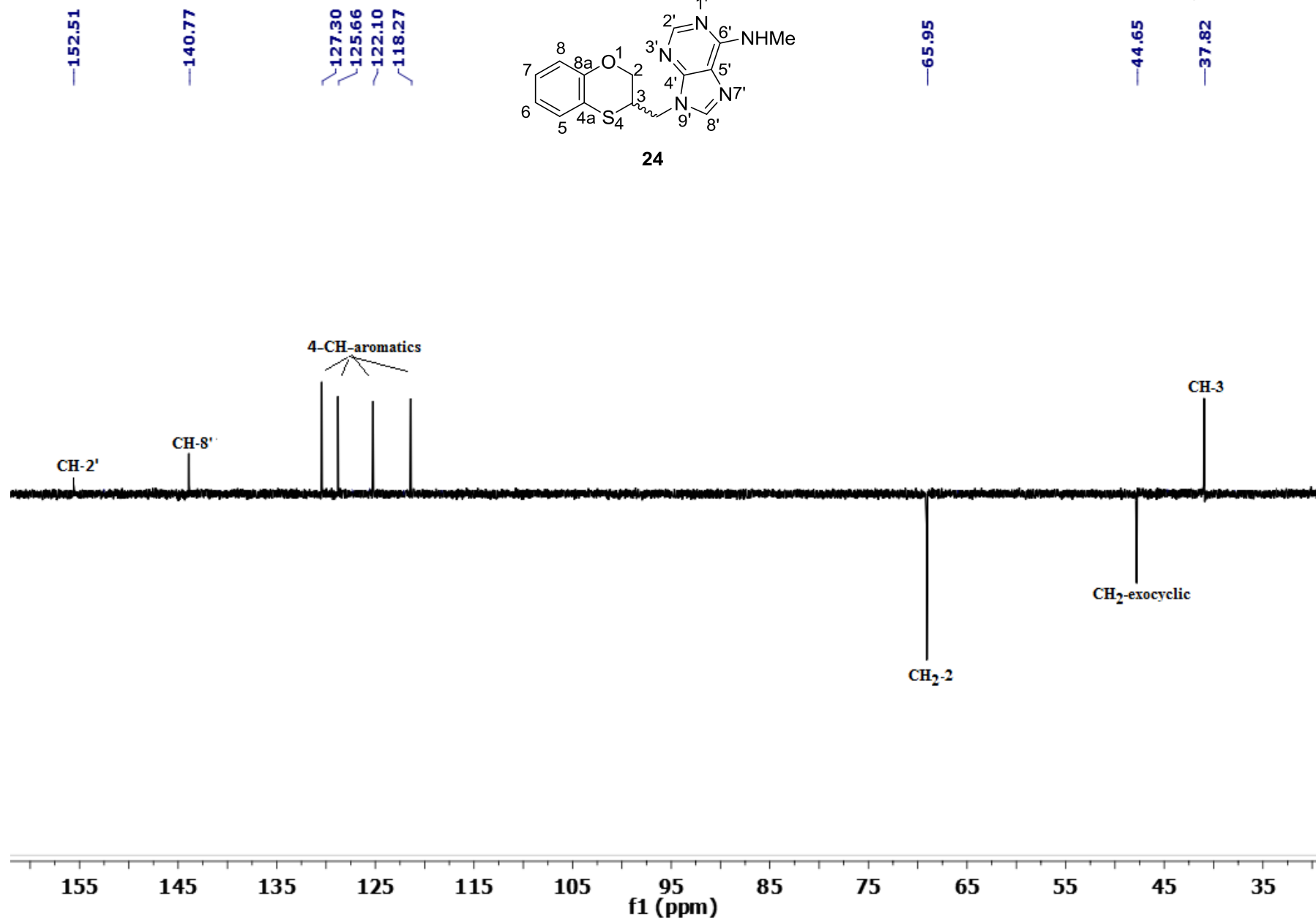
24

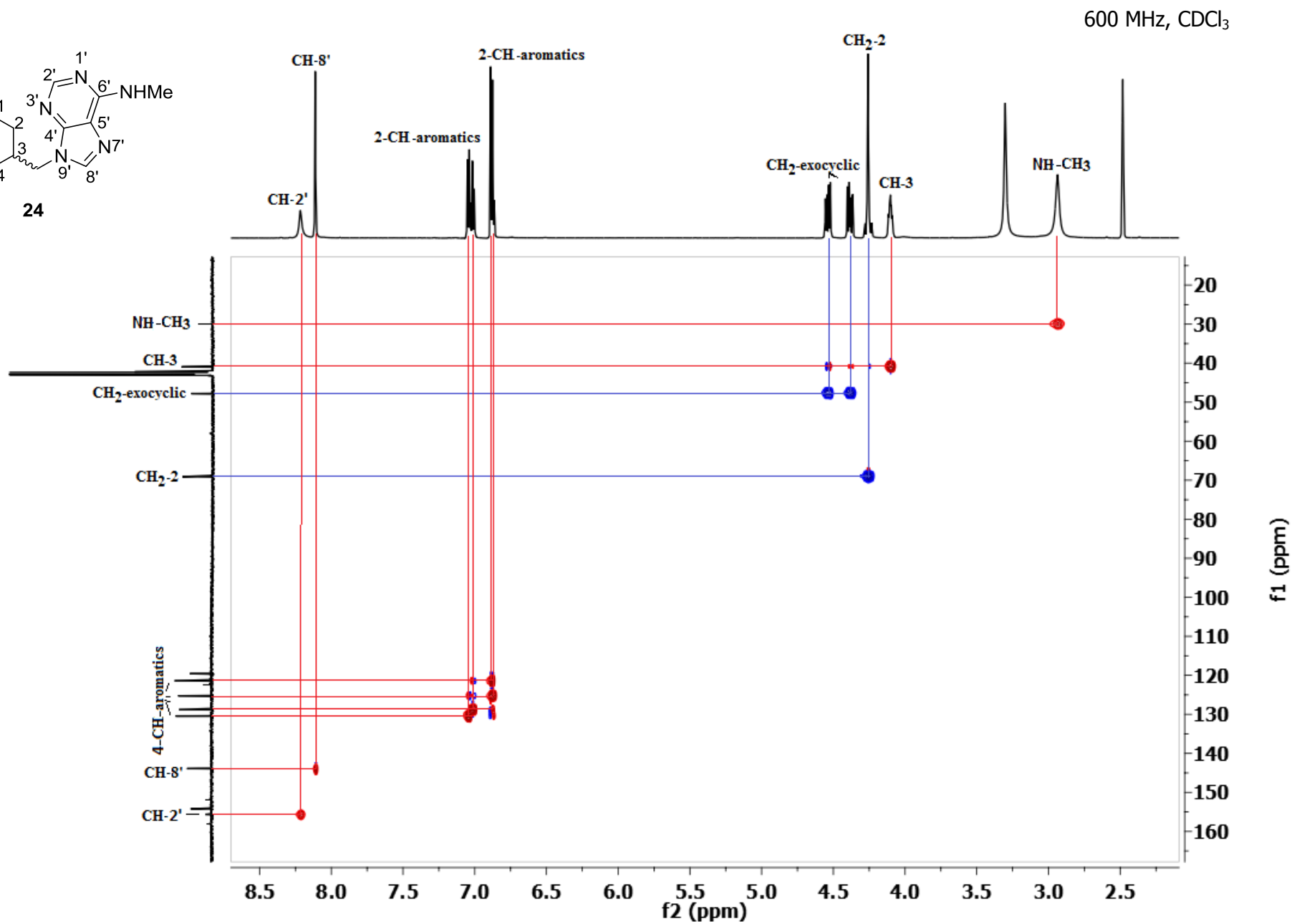
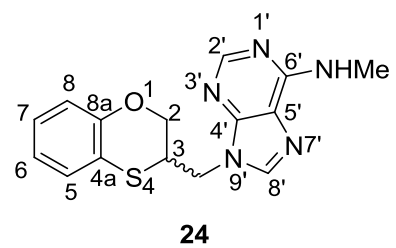


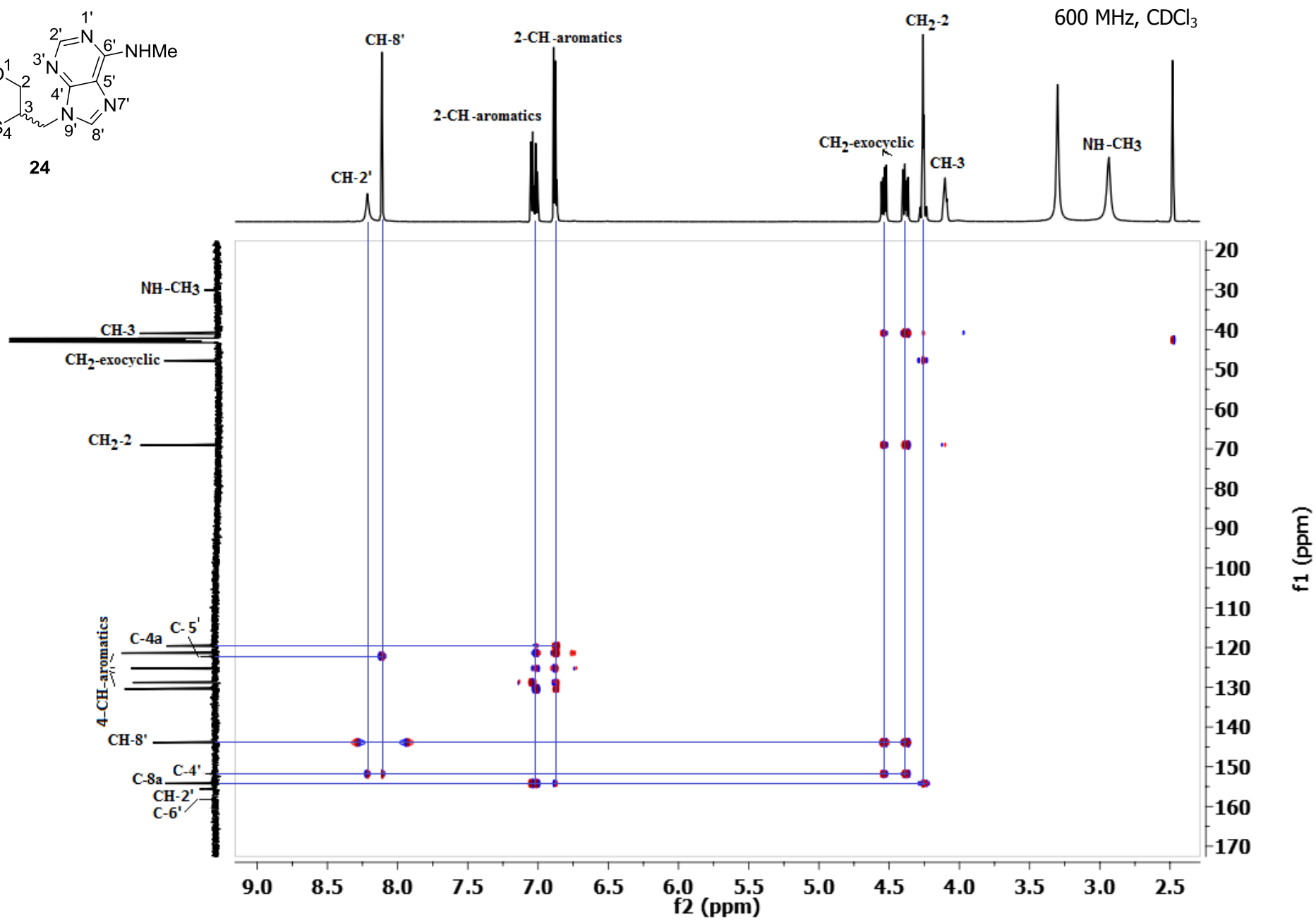
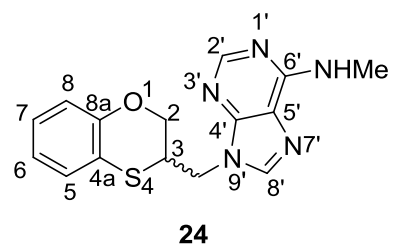


600 MHz, CDCl₃

24







Structure of (*RS*)-17

Figures S24 and S25 display the X-ray diffraction of (*RS*)-17. The crystal packing in (*RS*)-17 reveals that pairs of molecules form a dimeric structure by two symmetry-related $\text{C-H}\cdots\pi$ interactions involving the C10-H10A and the five-membered ring of the purine moiety of (*RS*)-17 ($\text{C-H}\cdots$ centroid distance: 2.90 \AA and $\text{C-H}\cdots$ centroid angle: 151.0°). In addition, there are additional $\text{C-H}\cdots\pi$ interactions connecting dimers involving the C22-H22B bond and the six-membered aromatic ring of the 2,3-dihydro-1,4-benzoxathiin moiety ($\text{C-H}\cdots$ centroid distance: 2.64 \AA and $\text{C-H}\cdots$ centroid angle: 166.0°). Therefore these $\text{C-H}\cdots\pi$ interactions build infinite chains. The cooperative effect of non-classical H-bond interactions ($\text{C22-H22A}\cdots\text{N1}$, 3.459 \AA and 149.0°) generates the 3D supramolecular architecture in the crystal.

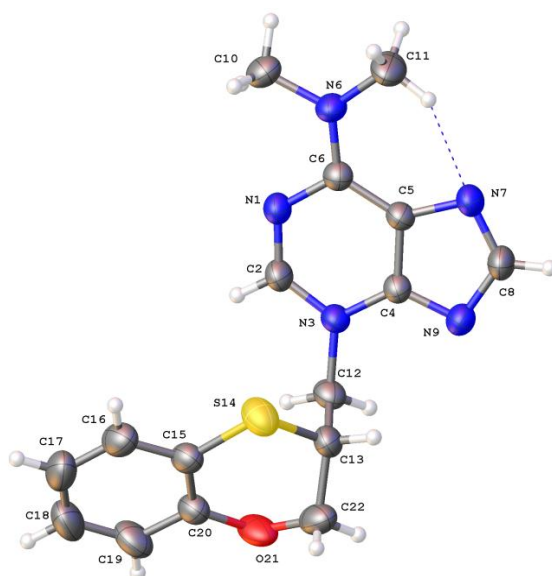


Figure S24. Molecular structure of (*RS*)-17. Hydrogen atoms are drawn as spheres of arbitrary radius. Ellipsoids of the non-hydrogen atoms are drawn at the 50% probability level.

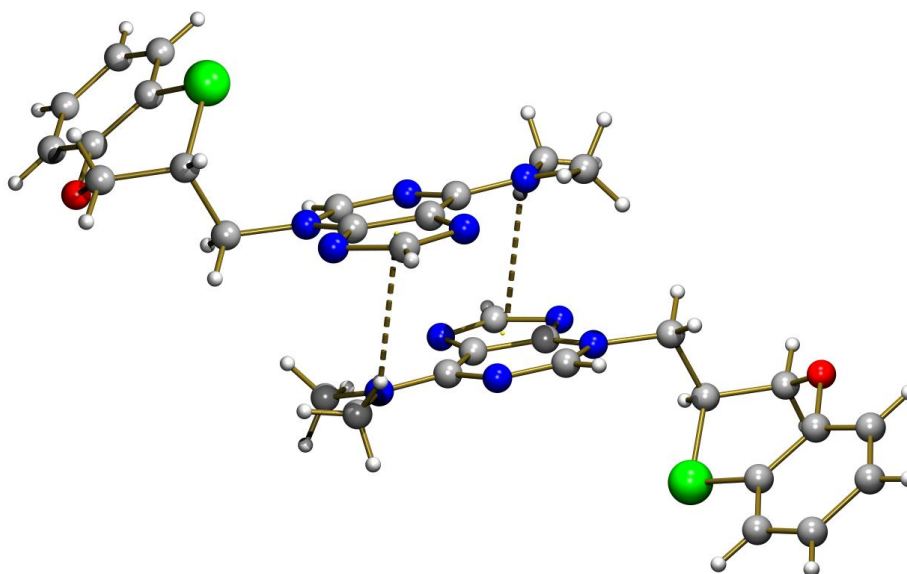


Figure S25. Detail of the dimeric structure of (*RS*)-**17** built by base pairing through --C-H \cdots π interactions.

Structure of (*R*)-**22**

Figures S26 and S27 show the X-ray structure of (*R*)-**22**. The crystal of (*R*)-**22** builds ribbons running along the *a* axis by intermolecular H-bonding interactions between adjacent (*R*)-**22** molecules by $\text{--N-H}\cdots\text{O}$ (2,3-dihydro-1,4-benzoxathiin moiety) interactions (2.985(5)Å, 139.64°). These ribbons are stabilized by $\text{--C-H}\cdots\pi$, involving the --C21-H21A bond and the six membered aromatic ring of the 2,3-dihydro-1,4-benzoxathiin moiety (C-H \cdots centroid distance: 2.62 Å and C-H \cdots centroid angle: 168.0°) and non-classical $\text{--C-H}\cdots\text{N}$ hydrogen interactions (C8-H8 \cdots N7, 3.311(6) Å, 153°). These ribbons are associated by $\text{--C-H}\cdots\text{Cl}$ interactions (3.559 Å, 125.11°) to build the 3D network.

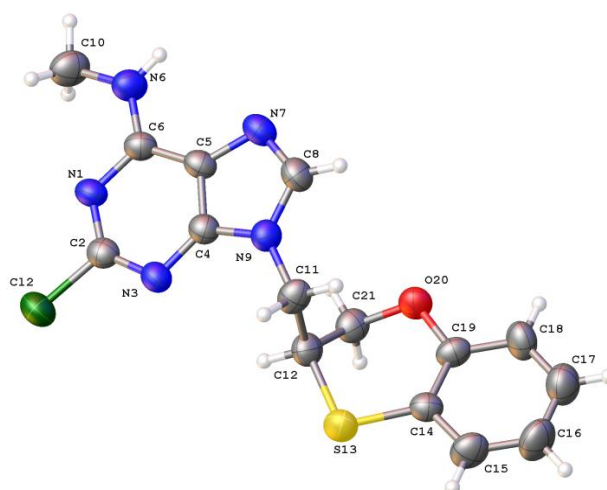


Figure S26. Molecular structure of (*R*)-**22**. Hydrogen atoms are drawn as spheres of arbitrary radius. Ellipsoids of the non-hydrogen atoms are drawn at the 50% probability level.

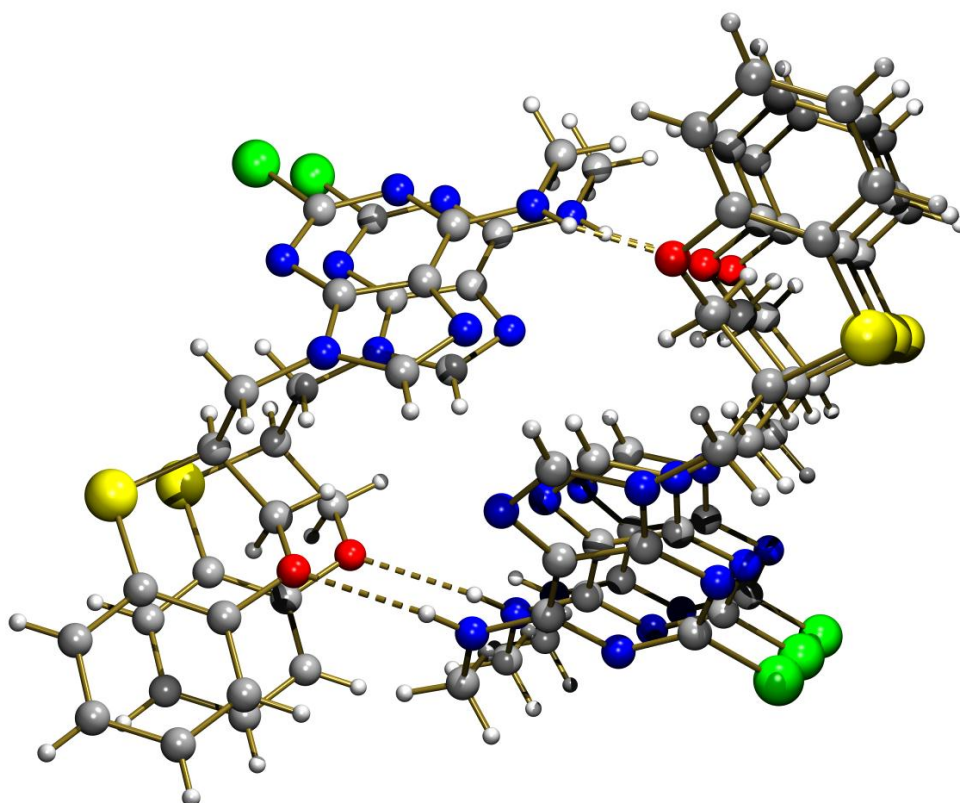


Figure S27. Fragment of a ribbon built by base pairing through -N-H \cdots O interactions

X-ray structure of (*RS*)-24

Figures S28 and S29 display the X-ray diffraction of (*RS*)-24. In the crystal of (*RS*)-24, pairs of adjacent (*RS*)-24 molecules are H-bonded by intermolecular symmetric interactions $\text{-N-H}\cdots\text{N}$ (imidazole) (3.07 Å, 149.0°). π,π -stacking interactions are observed between five- and six-membered rings (purine moiety) of anti-parallel neighbouring (*RS*)-24 molecules (centroid-centroid distances: 3.786 and 3.527 Å) connecting pairs and generating a ribbon structure running along the *a* axis. Ribbons are associated by $\text{C-H}\cdots\pi$ interactions (C-H \cdots six-membered aromatic ring of the 2,3-dihydro-1,4-benzoxathiin moiety: C-H \cdots centroid distance: 2.74 and 2.67 Å and C-H \cdots centroid angle: 161.0 and 173°) giving rise to two-dimensional frameworks parallel to the *ab* plane. Finally, additional C-H $\cdots\pi$ interactions involving the -C47-H47 bond and the six membered aromatic ring of the purine moiety (C-H \cdots centroid distance: 2.74 Å and C-H \cdots centroid angle: 173.0°) cooperate to reach the 3D structure.

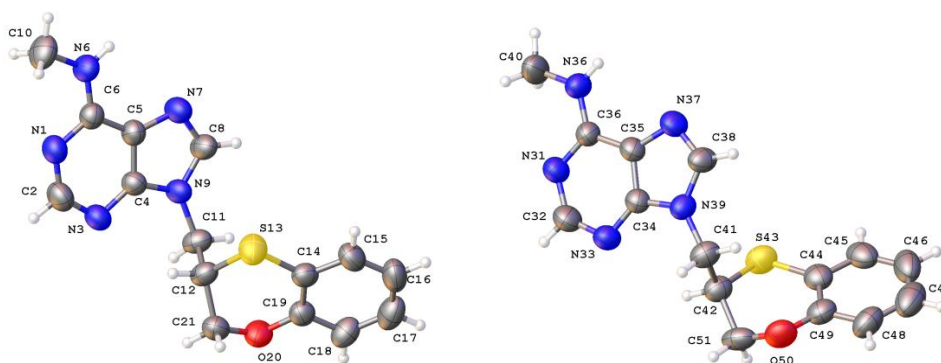


Figure S28. Molecular structure of (*RS*)-24. Hydrogen atoms are drawn as spheres of arbitrary radius. Ellipsoids of the non-hydrogen atoms are drawn at the 50% probability level.

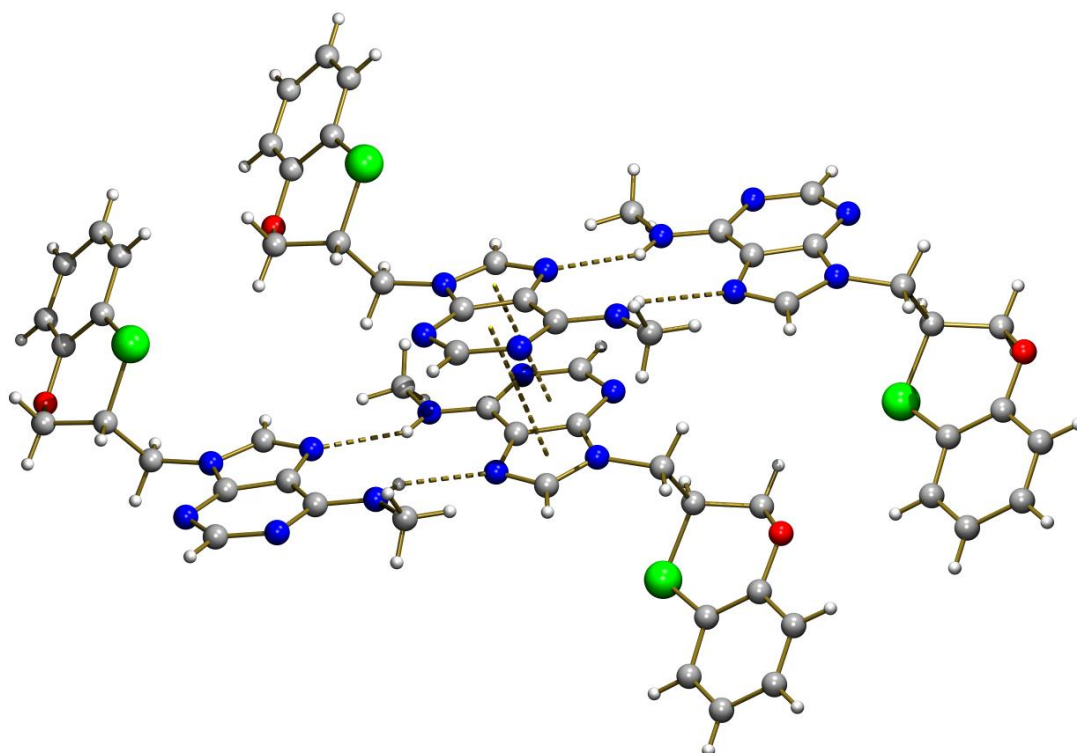


Figure S29. Fragment of a ribbon structure built by base pairing through symmetric N–H···N interactions and π,π -stacking interactions involving aromatic rings of the purine moiety of *(RS)*-**24**.

REFERENCES

- [1] BRUKER, APEX2 Software, Bruker AXS Inc, Madison, Wisconsin, USA, **2010**.
- [2] Sheldrick, G.M. A short history of SHELX. *Acta Cryst.*, **2008**, *A64*, 112–122.